PHOTODETACHMENT OF VARIOUS CONDENSED GASES AT LOW TEMPERATURES UTILIZING ULTRAVIOLET LIGHT

by

David C. Ellmann

A Thesis Submitted to the Graduate
Faculty of Rensselaer Polytechnic Institute
in Partial Fulfillment of the
Requirements for the Degree of
DOCTOR OF PHILOSOPHY
Major Subject: Heterogeneous Gas-Solid Kinetics

Rensselaer Polytechnic Institute
Troy, New York

June 1971

PHOTODETACHMENT OF VARIOUS CONDENSED GASES AT LOW TEMPERATURES UTILIZING ULTRAVIOLET LIGHT

by

David C. Ellmann

A Thesis Submitted to the Graduate
Faculty of Rensselaer Polytechnic Institute
in Partial Fulfillment of the
Requirements for the Degree of
DOCTOR OF PHILOSOPHY
Major Subject: Heterogeneous Gas-Solid Kinetics

Approved by the
Examining Committee:

P. Harteck, Thesis Adviser

H.A. Medicus

H.H. Richtol

R.R. Reeves, Jr.

Rensselaer Polytechnic Institute
Troy, New York

June 1971

CONTENTS

CONTENTS CONT'D

LIST OF TABLES

LIST OF FIGURES

LIST OF FIGURES CONT'D

ACKNOWLEDGEMENT

The author wishes to express his sincerest gratitude to Professor Paul Harteck for the opportunity of discovering the worth of numbers and for his patient advice.

The author acknowledges with grateful sincerity his many useful discussions with Dr. Robert R. Reeves, Jr.

A special thanks is extended to Mr. Roger W. Waldron for his often timely technical assistance.

The research reported in this dissertation has been sponsored in part by the National Aeronautics and Space Administration under grant number NGL 33-018-007.

Part 1

INTRODUCTION

A steady state equilibrium can exist between a gas phase and solid particles, with the gas adsorbing or condensing on the solid surface. Raising the temperature of the solid causes degassing and a new equilibrium can be reached.

At low pressures and under the influence of a high photon flux an additional factor for steady state equilibrium may be considered. If the photon does not simply result in a heating effect on the surface, but rather a quantum effect resulting in the ejection of an adsorbed or condensed particle by the photon, then the "evaporation rate" could be some fraction of the photons impinging on the surface.

The purpose of this thesis is to evaluate what quantum type effect of this nature may occur and under what conditions it may predominate. Of particular interest is the behavior of comets which, at considerable distances from the sun, receive a substantial photon flux, but possess an extremely low temperature. Particles rapidly orbiting the sun may sweep out large numbers of atoms over millions and even billions of years leading to an accumulation of interplanetary matter frozen on the surface. These are to be expected to be in the order of the nature of the "ices" referred to by Whipple.[1]

1.1 Evaporation Relations

The evaporation of molecules from a surface has indeed been a well explored concept. Values for removal of moles of gas as well as

values for removal of the last adsorbed layer have been both experimentally and empirically determined. In all these cases, the relation of evaporation to heat input has been the only criterion applied. Perhaps however, it is time to consider the concept that evaporation may occur in two modes: one a strictly thermal mode and the other a quantum mode. If this concept is valid, it might be expected that, since the quantum effect in evaporation is as yet undocumented, the magnitude of the thermal effect is much greater than the magnitude of the quantum effect. Thus, to detect and to subsequently study such a second mode evaporation, the conditions must be so controlled as to eliminate the larger effect and emphasize the smaller.

The conditions which immediately become apparent as affecting the determination of the quantum effect in evaporation are the temperature, the pressure, and the substance considered.

Perhaps the most critical parameter is the substance itself. While one may consider the evaporation of normal solids such as copper metal, it is only with extraordinary effort that one gets an evaporation of the metal by thermal methods. Theoretically, one could expect also a quantum effect in evaporation of copper metal, however this would, because of small magnitude of the thermal effect which is already the larger effect, require measurement of exceptionally small values. This is of course accepting as fact the ability to even demonstrate such an effect.

A much more reasonable substance would be one which normally was a gas and could therefore be caused to evaporate in large amounts

thermally and in measurable amounts by a quantum effect. A suitable gas would appear to be one of the condensible gases, some of which are listed in Table I along with their Van der Waals diameters, calculated attractive energies, and calculated Van der Waals constants.[2]

The second concern is the actual minimization of the thermal effect. This situation should be favorably attained as the temperature is lowered toward zero degrees Kelvin. At the freezing point of a gas, its translational and generally its rotational energies cease. Of course, as the temperature decreases fewer and fewer high levels of vibration are left available to the molecules. Thus the thermal evaporation effect becomes less effective simply because of the energy required to bring the molecules back to a normal energy content.

The factor of pressure enters as a matter of measurability. It is only reasonable that there is more precision in measuring a small quantity in a small quantity,than there is measuring a small quantity in a large quantity. So it is with the expected quantum effect in evaporation. Since the quantum effect is expected to be very much smaller than a thermal effect, it is best observed if a low pressure is the background for the measurement. Since the condensible gases chosen can have low vapor pressures (10^{-7} Torr or less) at liquid nitrogen temperatures both factors contribute to the third.

An idea of the magnitude of pressure change measured, is gained, if one assumes the following: 10^{14} photons strike the surface per second; the efficiency of the molecular detachment equals unity ($\varepsilon = 1$); no other event is occurring such as dissociation, or

Table I

Condensible Gases

Gas	$\varepsilon_o \times 10^{14}$ (ergs)	β ($\mathring{A}^3$)	$\alpha \times 10^{12}$ (ergs $\mathring{A}^3$)	d($\mathring{A}$)	M.P. (°K)
Ethane	14.25	110	15.68	3.74	90.1
n-pentane	21.89	240	52.54	4.88	143.6
1-pentane	22.08	200	44.16	4.60	108.1
NH_3	18.91	64	12.10	3.12	195.6
CO_2	14.16	72	10.20	3.24	194.8*
N_2O	14.44	76	10.97	3.31	182.5
SO_2	20.07	96	19.27	3.58	197.8
H_2O	30.13	52	15.67	2.91	273.3

*sublimes

Van der Waals $a = N_o^2 \alpha$

$b = N_o \beta$

$\varepsilon_o \beta = \alpha$

LN_2 77.5°K B.P.

$KT_{300°K} \cong 4.1 \times 10^{-14}$ ergs

$KT_{78°K} \cong 1.1 \times 10^{-14}$ ergs

recondensation on the surface; the volume concerned is 10^3 centimeters cubed; and the irradiation time is 10^2 seconds. A pressure of 1 millimeter mercury allows 3.3×10^{16} molecules/centimeter cubed. The irradiation above with its conditions would allow

$$\frac{10^2 \text{ sec.} \times 10^{14} \text{ photons/sec.} \times 1}{10^3 \text{cc.}} = 10^{13}$$

molecules/centimeter cubed or a pressure increase of $\frac{10^{13}}{3.3 \times 10^{16}}$ or $3. \times 10^{-4}$ Torr. Obviously, if the quantum efficiency is only a tenth instead of unity, the pressure change decreases by a decade down to $3. \times 10^{-5}$ Torr. Thus, noting that 10^{-5} is an upper limit of expected change, the background pressure would best be no higher than 10^{-6} Torr and still better be 10^{-8} Torr or less to insure the observation of the quantum effect.

Still another condition may effect the quantum effect. This has specifically to do with the transparency of the condensed gas to the impinging radiation. If the light is absorbed strongly, then only one or two monolayers may be concerned. However if many monolayers are needed to absorb the photon, then the surface may become important when its transparency to the irradiation is considered. The transparency concern allows several possibilities among which is multiple molecule eruptions. Part of this consideration too is the matter of preferential wavelength. Perhaps there is for each condensed gas a more effective photon. Too, this may or may not be part of the absorption character of the gaseous molecule.

1.2 Relation to Cometary Phenomena

The materials in interstellar space will have temperatures which extend from near zero degrees Kelvin to temperatures in thousands of degrees. Of primary interest however is the range between three degrees and one hundred degrees Kelvin. It is at these temperatures that solid particles may become condensation nuclei for interstellar volatile material.[3] As a first step, the volatile gases will be adsorbed on the solid particle as a monolayer. Further capture of the volatile gases will result in multilayering and eventually will result in a condensed phase.

In interstellar space there may exist, of course, conditions which forbid multilayering or even the formation of a monolayer. It is probably that vapor pressure and thermal conditions are extremely effective in controlling condensed gas buildup. But in addition, there may exist a highly selective photon impinging on the surface effect which causes molecules to evaporate from the surface in a manner analogous to electron detachment.

If, as a first approximation, one is allowed to assume that the distribution of solar wavelengths is, in interstellar space, very similar to the solar wavelengths distribution on Earth, then the temperature of a small particle can be directly related to the photon flux. The number of light quanta impinging on a particle to give the particle a definite temperature can be estimated using the Stefan-Boltzmann equation $R = \varepsilon \sigma T^4$ where R is the rate of energy emission per square centimeter, ε is the emissivity, σ is the Stefan-Boltzmann

constant and T is the absolute temperature. The rate can be converted to quanta per second by merely dividing by an energy per quanta number relating to a specific wavelength or average wavelength. The solar radiation in photons per square centimeter per second which strike the Earth and the estimated required number of photons needed to provide a particle with a surface area of one square centimeter with a temperature of 5, 15, and 25 degrees Kelvin are given in Table II as a function of full range and partial increments of solar radiance by wavelength.

To gain an insight into the position of a particle, relative to our Sun, having a temperature caused only by solar radiance, one may use the cometary particle temperature equation of Zanstra[4]; $T = (289)\ r^{-1/2}$ where T is the absolute temperature of the particle; r is the distance from the Sun in astronomical units. Table III lists several temperatures and distances at which they occur in astronomical units and miles.

If a multilayering process is to occur, condensible gas molecules must strike the surface of the solid particle. In a reduced atmosphere, the equation which relates the number of collisons on a surface to the number of molecules and their velocity, is applicable. The number of such particles N, hitting a square centimeter per second where A is the surface area, is given by:

$$N/A = 1/4\ n\ \bar{\omega} \qquad (1.1)$$

where n is the density in molecules per centimeter cubed and $\bar{\omega}$ is an estimated average molecular velocity (approximately 10^4 centimeters

Table II

Solar Radiation in Photons/cm^2/sec and
Related Particle Temperature

	Earth Temperature	Particle Temperature		
	300°K	5°K	15°K	25°K
Total Quanta	10^{17}	5×10^{9}	6×10^{11}	5×10^{12}
Quanta < 4000Å	10^{16}	5×10^{8}	6×10^{10}	5×10^{11}
< 2000Å	10^{14}	5×10^{6}	6×10^{8}	5×10^{9}
< 1800Å	10^{13}	5×10^{5}	6×10^{7}	5×10^{8}
L_α (1216Å)	10^{12}	5×10^{4}	6×10^{6}	5×10^{7}

Table III

Temperature of a Particle Related to
Its Distance from the Sun

Temperature (°K)	Distance (Astronomical Units*)	Distance (Miles)
5	3.34×10^{3}	3.1×10^{11}
10	8.35×10^{2}	7.8×10^{10}
20	2.09×10^{2}	1.9×10^{10}
50	3.34×10^{1}	3.1×10^{9}
70	1.70×10^{1}	1.6×10^{9}
90	1.03×10^{1}	9.6×10^{8}

* One astronomical unit equals 9.3×10^{7} miles.

per second at these low temperatures). Table IV gives the collision rate of condensible gas molecules as a function of the molecular density.

By comparing Table II and Table IV, it can be seen that, for certain ranges of molecular density and wavelength, the number of photon impacts on the surface and the number of molecule collisions with the surface are of the same order of magnitude. Therefore, the photodetachment of molecules from the solid particle surface would appear to be a critical parameter for the occurrence of monolayers, multilayers and condensed phases.

1.3 Molecular Photodetachment and the Photoelectric Effect

Electrons can be made to come off a filament simply by heating it. Also, the photoejection of an election was demonstrated as early as 1887 with the work of Hertz.[5] Perhaps in an analogous manner, the evaporation of molecules from a surface is both a thermal and a photo occurrence.

In considering the analogy of a molecular photodetachment phenomena to the photoelectric effect, there are parallels which necessarily might be cited. The first of these is the fact that a photoelectric current is directly proportional to the intensity of the irradiating light. One might then assume that the corresponding function in molecular photodetachment, the change in pressure, would also be directly proportional to the intensity of irradiation. This would appear to be a reasonable approach in that a quantum effect with its resultant efficiency would allow directly for an increase in the

Table IV

Collision Rate of Condensible Gases on a Surface as a Function of Molecular Density

Density (n) (molecules/cm^3)	Molecules Striking Surface (collisions/cm^2/sec)
10^4	2.5×10^7
10^3	2.5×10^6
10^2	2.5×10^5
10^1	2.5×10^4
10^0	2.5×10^3

variable as the number of photon occurrences increases.

Still another relatable equation might be

$$E = 1/2\ mv^2 = h\nu - p \qquad (1.2)$$

where E is the energy of the released electron, h is Planck's constant, ν is the frequency of the photon impinging, and p is a work function denoting the energy expended to free the electron from its position in the solid array. These quantities are immediately applicable to the photodetachment of molecules. The complex inter-molecule attractions and repulsions will not, it appears, allow a clear definition of a simple work function. But nonetheless, an equation can be written for the occurrence of photodetachment even if the factors are complex. The energy of the detached molecule will still be equal to the energy of the photon minus the work function which now may include the excitation of molecular energy levels as well as the energy necessary to free the molecule from its surrounding neighbors. In any event, even these complex factors may serve as identifying characteristics of specific condensed gases.

When E = 0, in the photoelectric effect, the wavelength of the incoming photon is just sufficient to eject an electron with zero velocity. By strict analogy, one would expect that there is also a wavelength which would just allow molecular detachment from a surface. It is this point which may not be exact. It may be possible to find a wavelength which does with some efficiency detach a molecule. If the wavelength were increased, the frequency and therefore the energy decreased, one could expect a change in the detaching process. This

assumes that the threshold does exist and will operate. Of course, this need not be so, and an alternative would be that the detachment process still occurs but in a lesser degree. The opposite point, that of increased photon energy, would correspondingly require an increased photodetachment effect.

Still another point is that the energy of the photoelectron is independent of the irradiation intensity. This would indicate that a single photon interaction would be responsible for a single electron. If multiple photon interaction would be allowed, then by equation 1.2 , the resulting energy of the electron would increase since the work function would remain the same. This is not experimentally true, thus a single photon would seem responsible. This however would need not be the case for molecules. In diatomic and especially polyatomic molecules, it is not difficult to visualize a situation in which some vibrational level is reached by single, double or multiple photon interaction before a detachment could occur. It might be even considered that when a certain level of photon energy is reached several molecules may be detached.

The differences considered are so done, not to negate the analogy, because it could be valid, but rather to point out that molecules of condensed gases fit neither an ideal model nor an electron model with any great deal of agreement.

The concept of molecular photodetachment to date had not been investigated. It does however offer the opportunity to examine the behavior of condensed gases at both low pressures and low

temperatures. The magnitude of the effect, its wavelength dependence as a function of the gas condensed, temperature dependence if any and the kinetics of the photodetachment are only a few of the possible results valuable to cometary phenomena as well as to the understanding of intermolecular forces.

Part 2

EXPERIMENTAL APPARATUS

2.1 Photodetachment Cell

A suitable photodetachment cell has been constructed. A schematic of its major parts is given in Figure 2.1 and a larger side-view of the pyrex surface and window is given in Figure 2.2. Figure 2.3 is a photograph of the apparatus.

The apparatus itself is a modified dewar. A part of its inner wall has been replaced by a flat circular pyrex surface with an area of 1.3 ± 0.1 square centimeters. The outer wall has also been modified. As shown in Figure 2.2 there is a cupola attached to the outer wall in such a way as to align a quartz window directly opposite and parallel to the pyrex surface. The window is made of quartz with 85% transmission of 2000Å light for a one millimeter thickness. The window is 3 millimeters thick and 2.5 ± 0.1 centimeters in diameter. Around the pyrex surface and extending toward the quartz window is a flare or collar. This collar approaches the window mount to within a millimeter. The intent of the collar is to isolate the actual cell volume from the volume between the dewar walls. At a pressure of 10^{-8} Torr or less, effusion processes dominate and so, the rate of mass transfer to the dewar volume from the cell volume is very minor. Three function tubes are directly connected to the window cupola in such a position as to expose a maximum cross section of the tubes to the cell volume and a minimum cross section to the dewar volume. Each of the three function arms has a purpose. The one tube contains the ionization

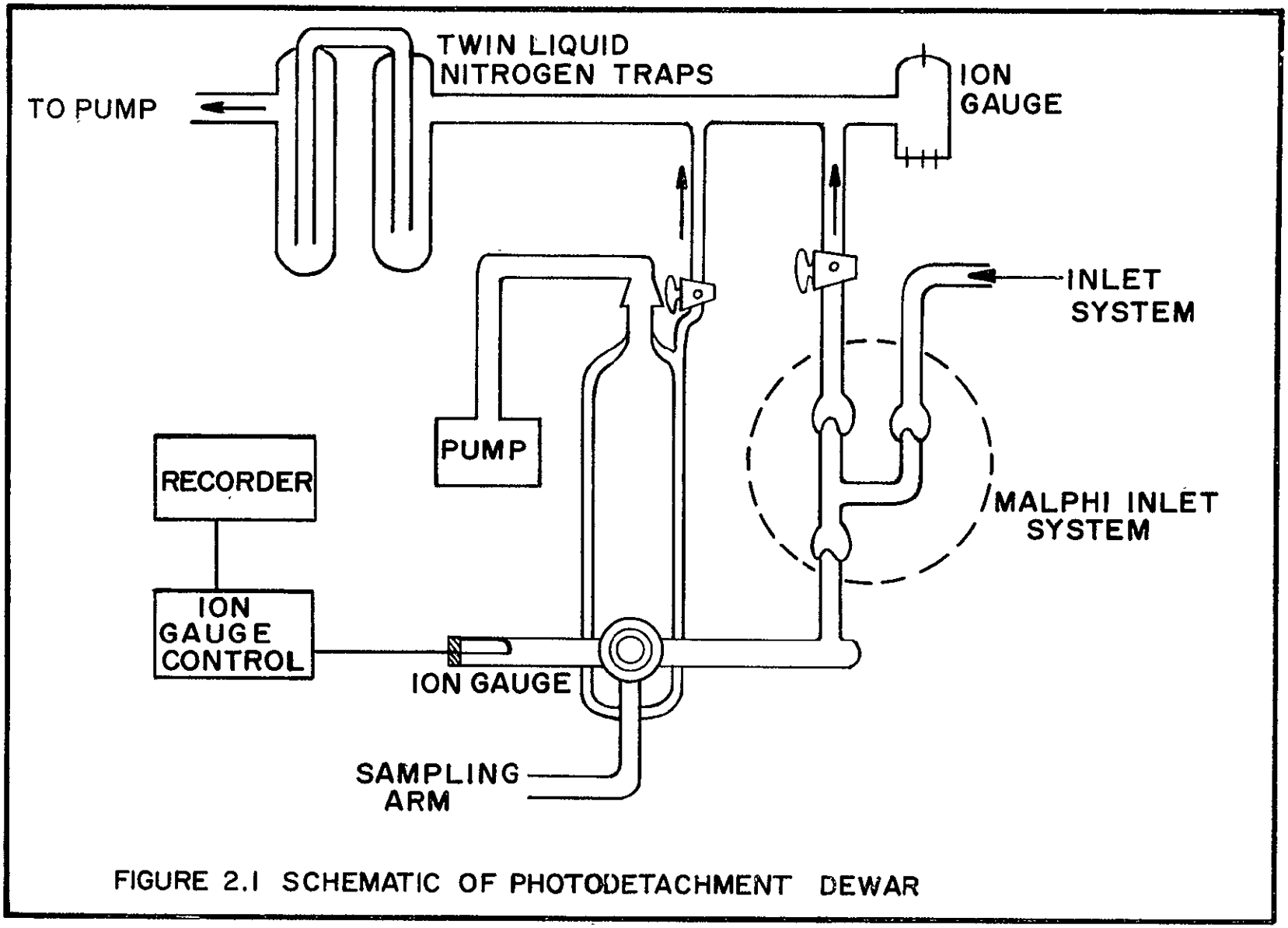

FIGURE 2.1 SCHEMATIC OF PHOTODETACHMENT DEWAR

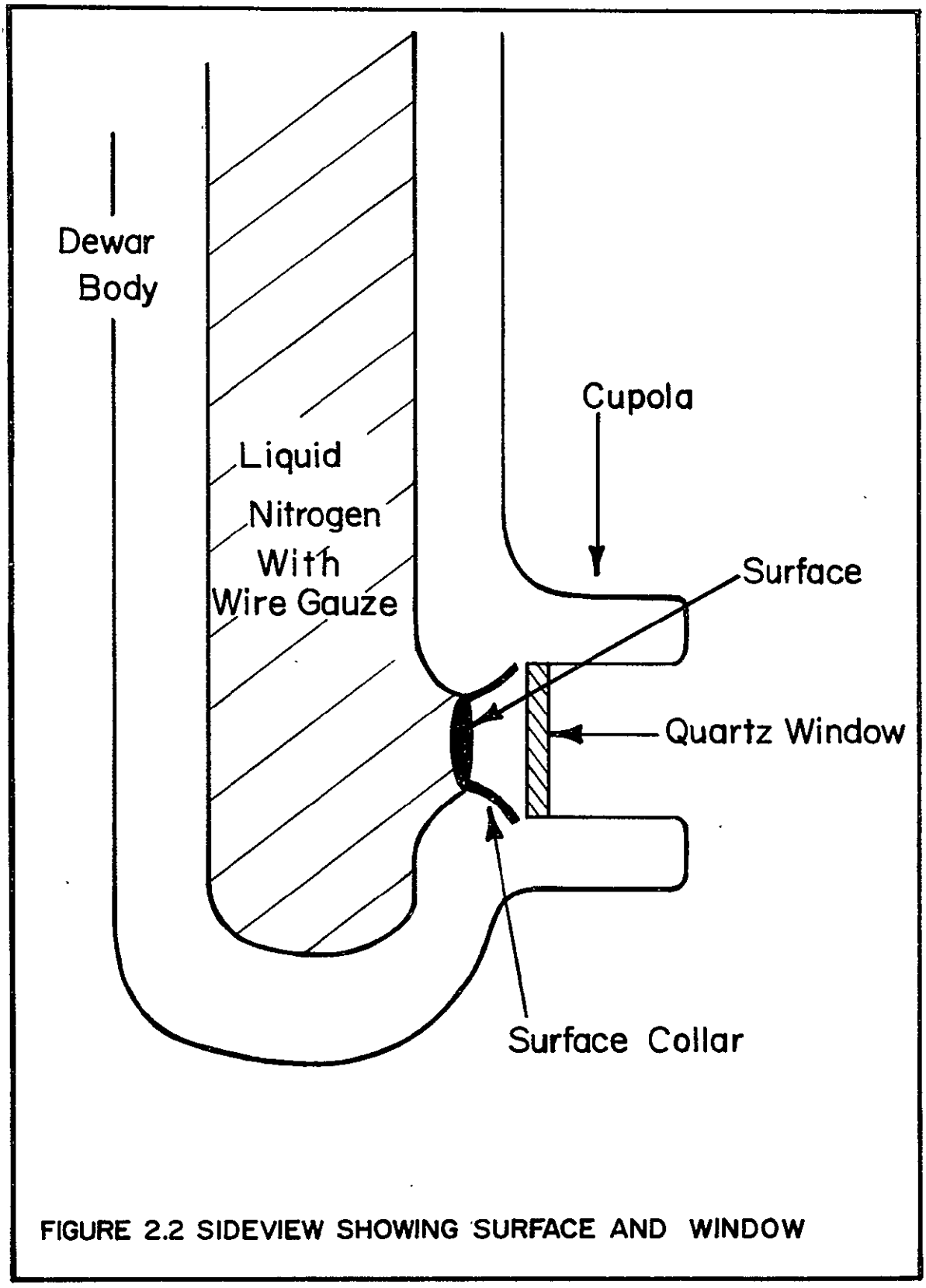

FIGURE 2.2 SIDEVIEW SHOWING SURFACE AND WINDOW

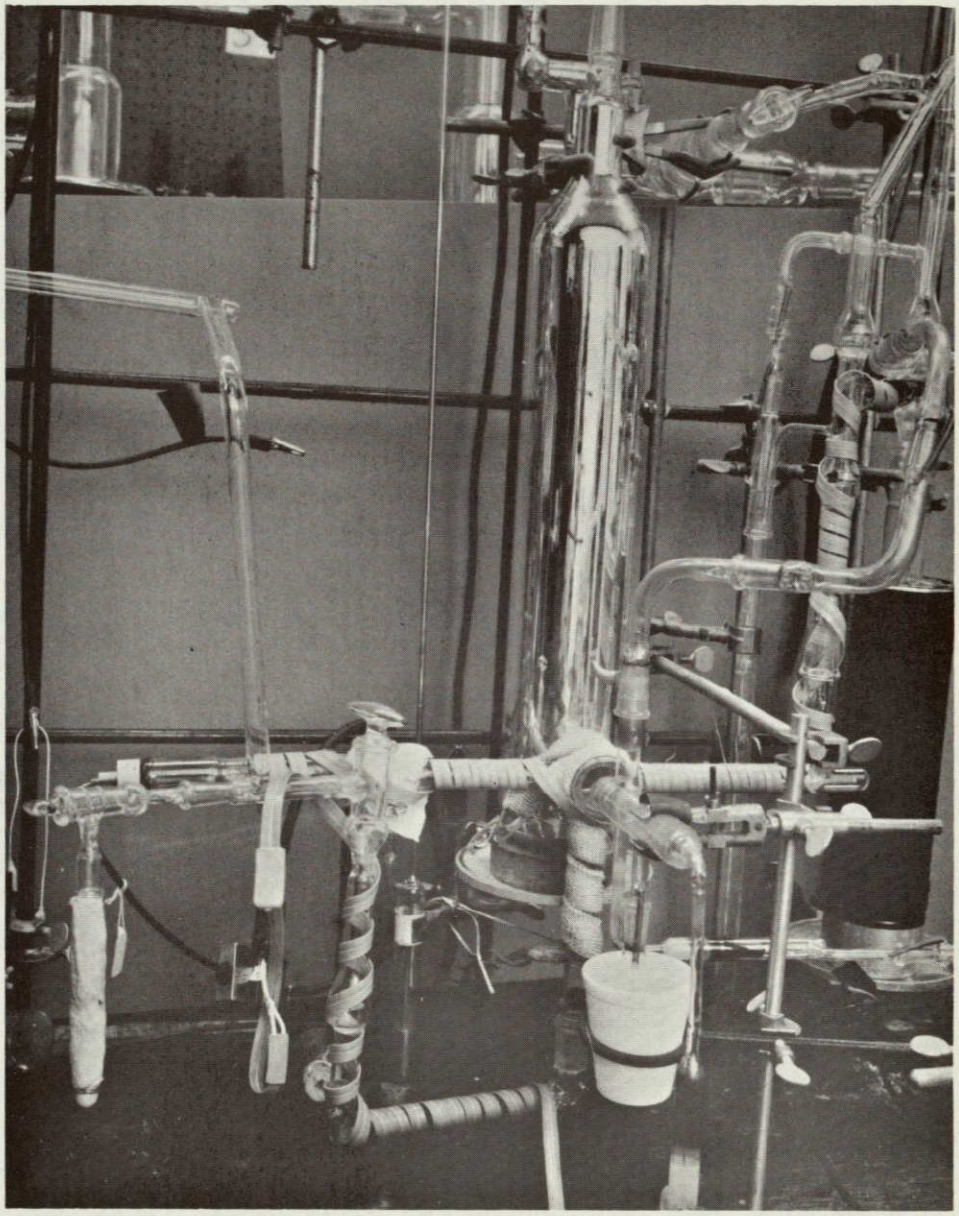

FIGURE 2.3 THE PHOTODETACHMENT SYSTEM

gauge; the bottom function tube connects to a sampling volume; and the third function tube connects the photodetachment volume to both the pump system and the gas storage volumes through a system of valves.

The photodetachment volume itself is isolated from the pumping system and the sampling zeolite by several all pyrex sliding MALPHI valves. The locations of the MALPHI valves are shown in Figure 2.4.

2.2 Pumping System

The 10^{-8} Torr pressure in the photodetachment system is maintained by the use of a mechanical pump and a mercury diffusion pump. The rough pump is a model 1402-B by Welch. It has a free air displacement of 140 liters per minute. The diffusion pump is the Consolidated Vacuum Corporation's Model MGH 50-02 with a pumping rate of 50 liters per second below 10^{-3} Torr. The three function tubes up to the MALPHI valve, as well as the window cupola, are kept at a constant 378 degrees Kelvin by heating tapes regulated with a Variac "Autotransformer" model W5MT3 rated at 0-140 volts output.

2.3 Pressure Monitoring System

The pressure inside the photodetachment system as well as the pressure change caused by irradiation of the condensed phase with ultraviolet light were measured using a Consolidated Vacuum Corporation Model GIC-200 ion gauge controller and a Bendix Corporation small volume ion gauge Model GIC-028-2. The controller was used at its 2 amps full scale setting to prevent gettering by the filament. The stability

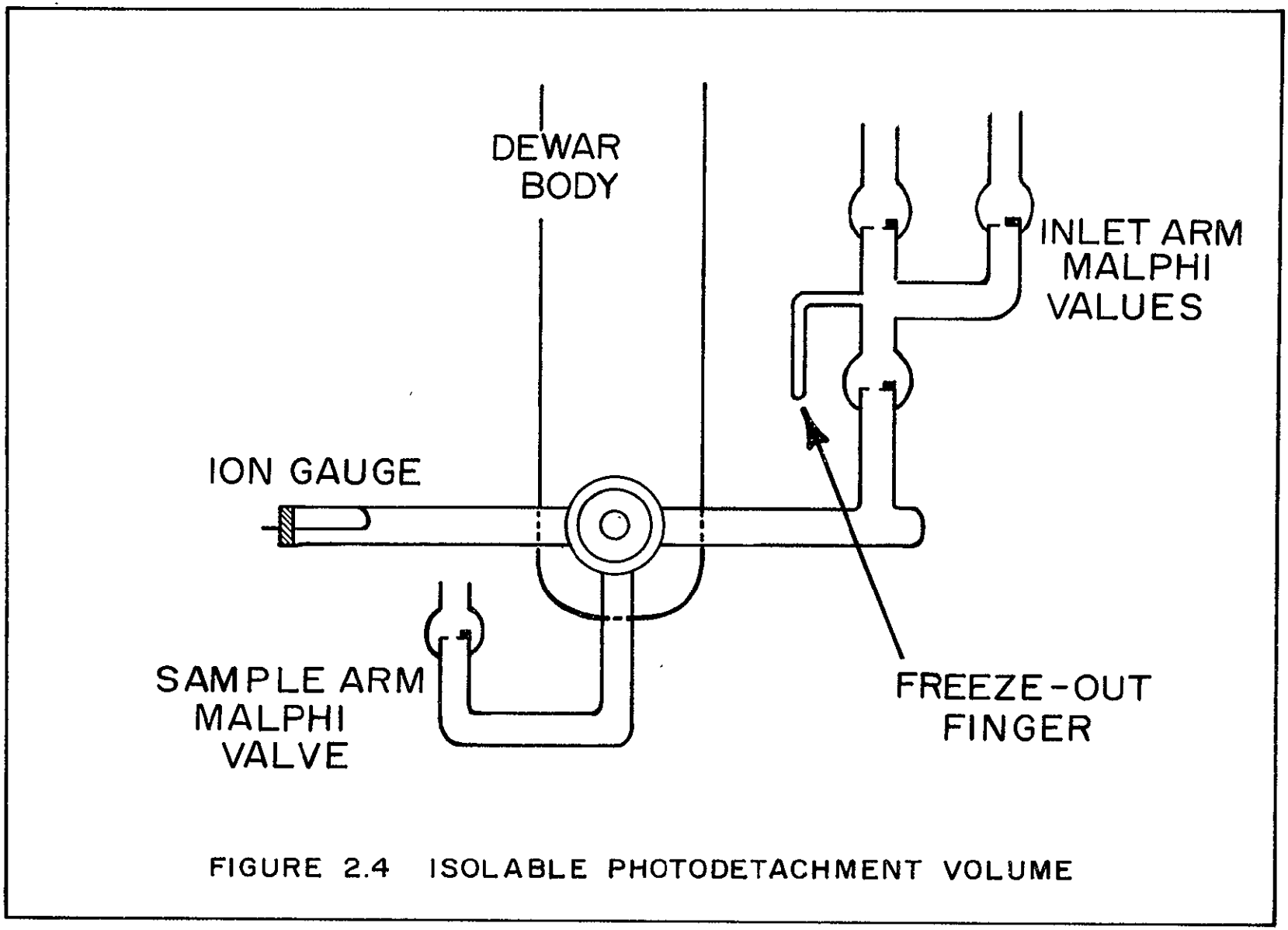

FIGURE 2.4 ISOLABLE PHOTODETACHMENT VOLUME

of the controlling unit amplifier is given as being within 1 percent and the emission stability is given as being within 2 percent. The 10 millivolt full scale output was recorded on a Moseley "Autograf" Model 7100B strip chart recorder. Both channels of the recorder were fitted with Model 17501A modules supplied by the Hewlett Packard Company. In most instances, the recorder was operated in its 10 millivolt full scale setting.

The pressures within the auxillary vacuum rack were measured, in the range 10 Torr to 10^{-4} Torr, by means of a Model 530 Alphatron manufactured by the National Research Corporation. For pressure measurements above 10 Torr but less than 700 Torr in the auxillary vacuum system alone, mercury stick manometers are used to monitor gas transfer and supply.

2.4 Temperature Control of Condensing Surface

As was illustrated in section 2.1, the condensing surface is located in the inner wall of the system's dewar (see Figure 2.2). Thus by filling the dewar with liquid nitrogen, the surface is put into contact with the liquid. In turn, the surface is cooled to 77 degrees Kelvin and gases can be condensed on it. The cooled pyrex surface temperature was controlled by varying the temperature of the liquid nitrogen. The liquid nitrogen temperature was varied by varying the nitrogen pressure according to the vapor pressure curve. A desired pressure of nitrogen was maintained at less than one atmosphere by using Welch Model 1400 mechanical pump having a free air displacement

of 25 liters per minute. The pumping rate was regulated by means of a 10 millimeter vacuum stopcock located within a foot of the pump inlet. The stopcock is located at this point to prevent its being frozen by the passage of the still cold nitrogen gas pumped from the dewar. The output of the pump was measured with a Matheson flowrator Model #602. The resulting pressure within the dewar was measured with a mercury stick manometer.

2.5 Ultraviolet Sources

Three different ultraviolet light sources were employed in this investigation. On was a conventional mercury vapor discharge lamp made by Englehard Industries, Hanovia Lamp Division. This lamp was used as a source of 2537Å irradiation. The two other sources were iodine lamps and provided 2062Å photons.[6] These last two lamps were developed and tuned for maximum 2062Å photon output in this laboratory.

The iodine-argon lamp was the lamp primarily used. It was a flow lamp, which balanced the pumping rate of a Welch Model 1400 mechanical pump 25 liters per minute, against a flow of Matheson pre-purified argon gas regulated by two Matheson #602 flowrators. Figure 2.5 gives the lamp and its system. The iodine used was Fisher Brand A.C.S. grade. It was used without further purification or drying since the system was a flow system and after a short time, the argon gas carried off most of the interferring water. The lamp was powered by a 800 watt, 0-150 volt A.C. (output) transformer. The output voltage and power were varied by a Variac Model V10 feeding the primary of the high voltage transformer. Power dissipated in the lamp was measured

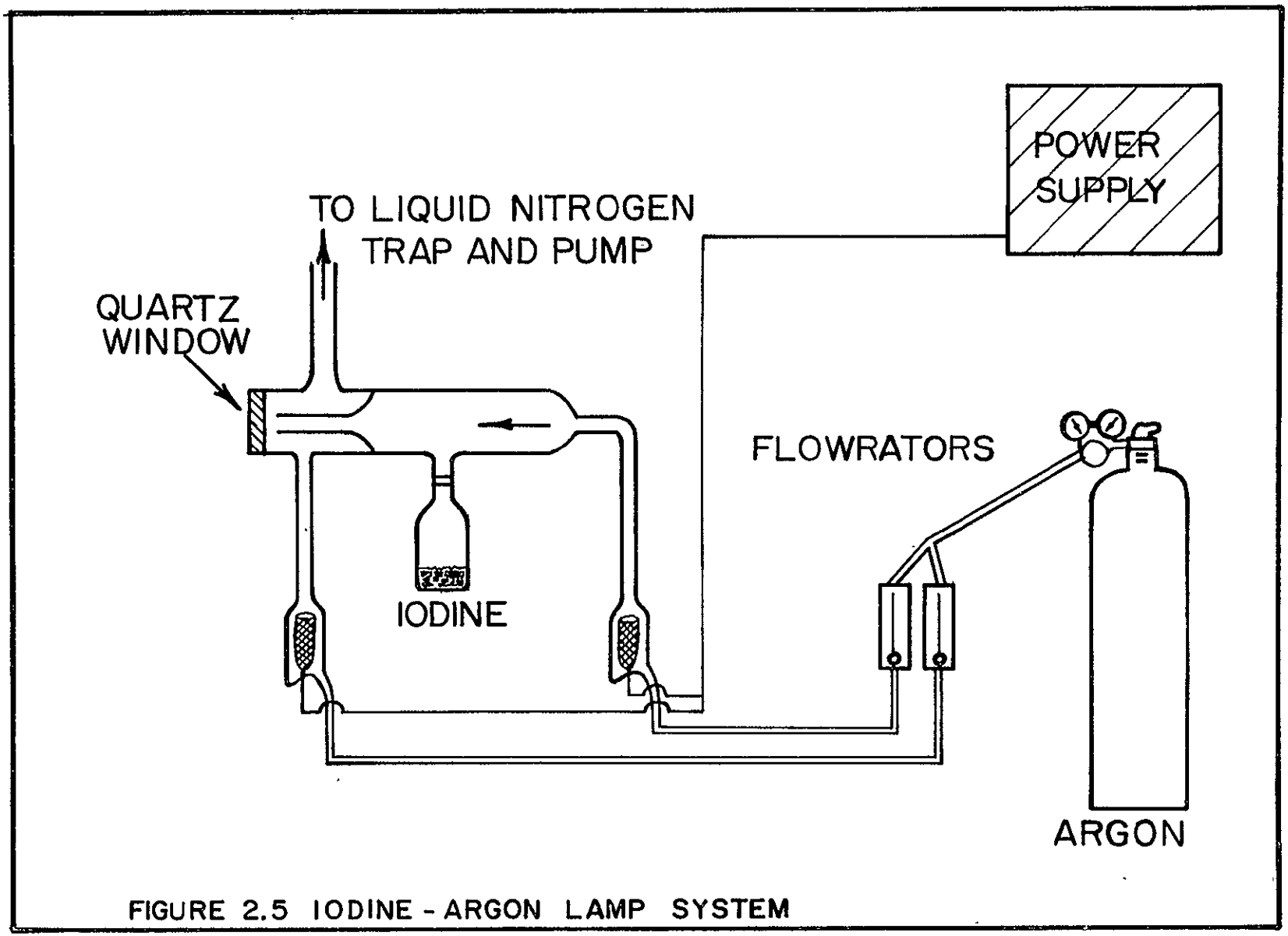

FIGURE 2.5 IODINE - ARGON LAMP SYSTEM

by observing the power supplied to the transformer primary indicated by a wattmeter. The lamp face was made of quartz from Quartz Scientific. It was 3 millimeters thick and 2.5 centimeters in diameter. It has the same transmission characteristics as the dewar window, i.e., 85% transmission of 2000Å light at a thickness of 1 millimeter.

The second iodine lamp was a radio-frequency closed volume iodine lamp designed in this laboratory. (The radio-frequency iodine lamp will be referred to as the RF lamp and the iodine-argon lamp simply as the iodine lamp.) This lamp was used for all the early work of this photodetachment system. As seen in Figure 2.6 the lamp again has a quartz face with 3 mm thickness and 2.5 centimeter diameter but, its body is composed of the graded seal from the window tapering down to 18 millimeter O.D. pyrex tube and finally to a 1 millimeter I.D. capillary. The iodine used was Fisher Brand A.C.S. grade. However, for the closed volume lamp, the iodine was first vacuum distilled. In doing so, the many small crystals with their adsorbed water became large crystals in another vessel but without the high water content. This process was used still again to introduce the iodine into the lamps through the capillary end. Once sufficient iodine was present in the lamp, the lamps were repeatedly filled with dry argon and then pumped out again. During this drying process, the new lamp was subjected to radio-frequency discharge to further dry the interior surface and the iodine. Once the discharge was seen to be free of water as noted by the lack of 3064Å OH band emission, the lamps were sealed off and fitted with the antenna harness.

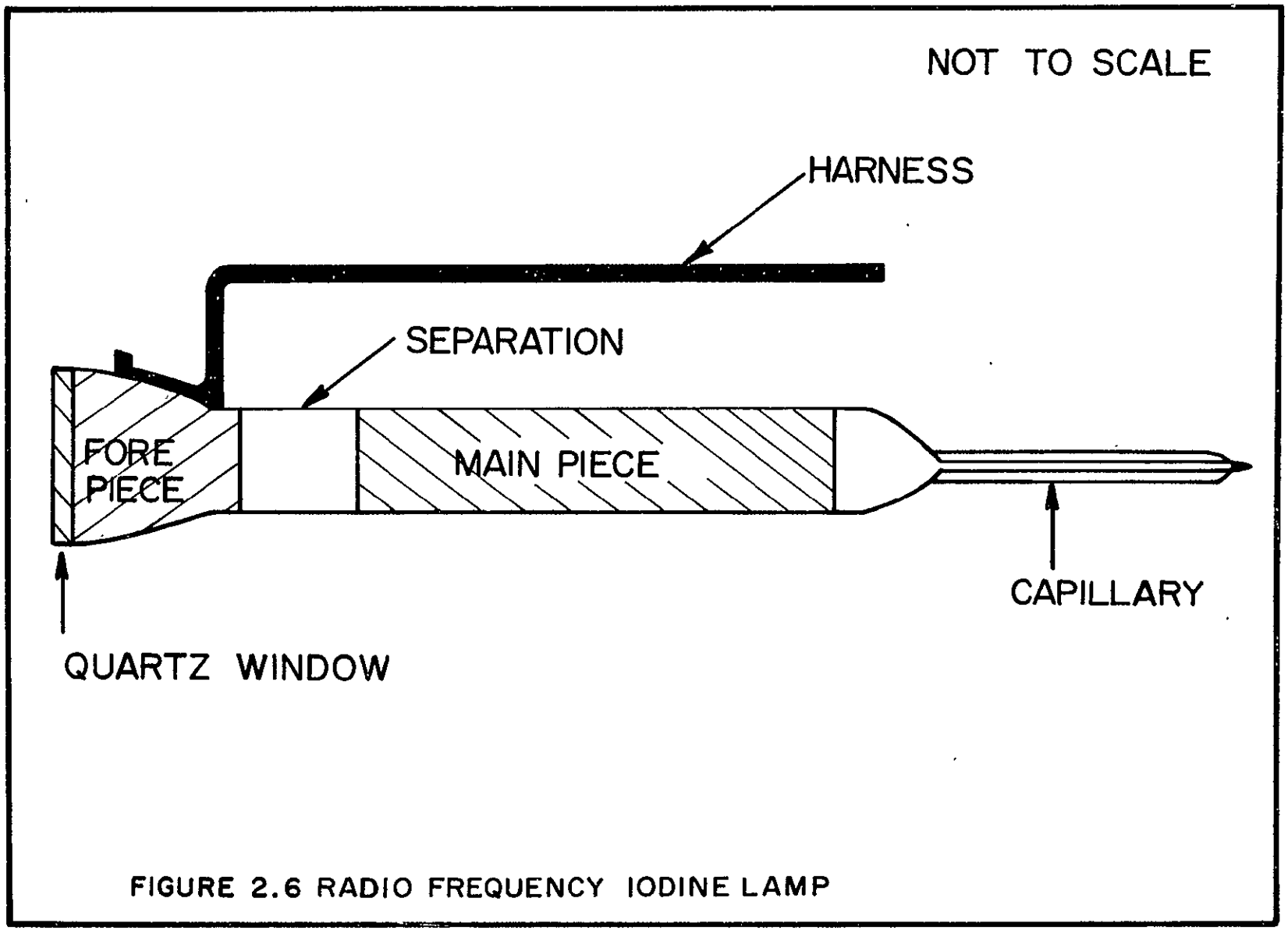

FIGURE 2.6 RADIO FREQUENCY IODINE LAMP

Initially, the lamps used a 20 turn-coil winding of #18 bare copper wire on the main body. Used with this was a harness 4 centimeters away from the body and contacting the body at both ends of the winding without touching the winding itself. This design gives a plasma centered within the lamp.

Knowing that self absorption of the emitted light by iodine atoms could reduce the output intensity, the harness was changed. This time only a single connection to the body was used; the connection to the body at the capillary was deleted. This change moved the plasma to a position very near the window. Subsequent variation of the length of the single harness showed that although there was no noticeable intensity change, the output became less stable as the length was decreased. Finally, a single harness of #18 bare copper, 25 centimeter long, at a distance of 4 centimeters from, and parallel to the main body was used.

One annoying factor of the lamp as so far described was the extreme heating of the copper windings. To alleviate this, aluminum foil was wrapped around the main body as a replacement for the copper coil where the coil had been positioned. Immediately, the heating became less.

With the aluminum in place, it seemed logical that there might be some maximum value for weight or type of main body metal. Tin and lead foil were tried as well as the aluminum foil. The first two gave lesser intensities so they were not pursued. The aluminum foil was varied from 64 square centimeters to 512 square centimeters. In a

well coupling Kilocycle range, the amount of aluminum foil did not appear to matter. Consequently, the final lamp has a 256 square centimeter main foil.

The lamp has three distinct segments. The fore piece, onto which was connected the harness; the main piece and the separation between these two. In way of finding the best placement, the separation between the fore and main pieces was also varied. Admittedly, the variation can only be between 8 and 1 centimeters, but nonetheless, the intensity does vary significantly. The lamp now has a 4 centimeter separation between the fore piece and the main piece.

The optimum fore piece length, 4 centimeters, was also determined through variation. As the size was increased, the plasma moved away from the window and the intensity decreased.

Still more variables of this lamp are the transmitter, the band width, and the frequency. For these lamps, increased transmitter power increases the intensity but also increases the temperature and decreases the lamp life. Concerning the band width of the transmitter, greater success was achieved at more and varied frequencies using the 6 meter band for the aluminum main piece lamps and 15 meter band for the copper wire main piece lamps. The following frequencies were tried with all band combinations: 8388, 7192, 7079, 7064, and 3701 Kilocycles. The frequency most effective for the lamp of these dimensions was 7192 Kilocycles. The transmitter used was a Model HT-40 Hallicrafter intermittant transmitter adapted for continuous 75 watt operation.

The finished lamp developed a very constant output in the order of 10^{15} photons per second/lamp face of 2062Å light. A comparison of the character and output of the two iodine lamps is given in Table V.

The optimization of conditions for maximum output of 2062Å photons of both lamps, the iodine-argon and the radio-frequency iodine, were measured using a Jarrell-Ash grating scanning monochrometer (Ebert 82-000) with its companion recorder Model 82110 (Bristol).

2.6 The Condensable Gases

Each of the gases examined for photodetachment phenomena were taken from commercial preparations available from the Matheson Corporation. The gases were each fractionally vacuum distilled until, by mass spectrometric analysis, they exhibited no large foreign gas content.

2.7 Detached Species Sampling

The method used for detached species analysis was that of zeolite at liquid nitrogen temperature. The zeolite was Linde Molecular sieve 5A in pellet form. However, before use, the zeolite was washed with concentrated hydrochloric acid, rinsed with distilled water, heated to 350° centigrade in a muffle furnace and finally heated to 200° centigrade under vacuum of 10^{-4} Torr.

The mass spectral analysis was carried out on a Consolidated Electrodynamics Corporation Model 21-130 Mass Spectrometer. This machine was used with a daily calibration of gases being measured. The resultant reproducibility was within 0.1%.

Table V

Lamp Comparison

		I_2-AR	RF-I_2
1)	Physical Set Up	Complex	Simple
2)	Intensity Variance	5%	< 5%
3)	Intensity (Maximum)	10^{15} photons/sec	10^{15} photons/sec
4)	Power Required	200 Watts	75 Watts
5)	Electrical Disturbance	(none)	Some if not properly set up

Part 3

EXPERIMENTAL PROCEDURE

3.1 High Vacuum System

The high vacuum, in the range of 10^{-9} Torr, needed for the observation of the photodetachment effect, was obtained using a series of vacuum pumps. The pressure within the system was of two aspects, first the non-condensible gases and second the gases adsorbed on the walls of the system. The noncondensible gases were removed by continuous pumping. The adsorbed gases were removed by maintaining the walls of the detachment vessel at 378 degrees Kelvin while the pumping continued. Typically, after several days of pumping and heating, the pressure within the photodetachment volume was reduced to 6×10^{-9} Torr. This was the value accepted as a beginning pressure i.e. the pressure just prior to the addition of gas to be deposited on the cooled pyrex surface.

3.2 Gas Inlet Procedure

The transfer of the purified gases into the detachment system required an auxillary vacuum apparatus. This auxillary apparatus served as both a gas storage volume and a calibrated volume for precise gas measurement. The gases were measured in terms of the number of molecules necessary for the experiment by filling a known volume to a specific pressure. The absolute pressure was determined by using an Alphatron and applying the manufacturer's "specific gas multipliers".

The gases, since they are condensible, were transferred by multiple condensations at liquid nitrogen temperature. The loss of gas from the original measured value per condensation can be estimated as 0.01%. Of course this loss is dependent upon the vapor pressure of the gas concerned at liquid nitrogen temperature. To prevent loss of the gas by adsorption to the walls while being transferred, the volumes through which the gases were to be moved, were preconditioned with the same gas as was being transferred. Usually two condensations were used to bring the gas within the photodetachment volume and the third condensation occurred as the gas was deposited on the cooled pyrex surface of the photodetachment cell.

An interesting point to note is that after the gas was initially deposited on the surface, the cryodeposit continued to age or come to an equilibrium condition. This was seen with all the gases, but more pronounced with carbon dioxide. This effect was evidenced by the decidedly different detachment values observed as the surface changed with time. After several hours, the detachment values stabilized.

3.3 Ammonia Calibration of 2062Å Line

The method used for the calibration of both the RF lamp and the iodine lamp was an ammonia photodecomposition reaction. As can be seen in Figure 3.1, ammonia exhibits a fairly strong absorption of the 2062Å line. The actinometry was carried out using a gas mixture 0.09 mole fraction argon with the remainder pure dry ammonia. In all calibrations, the same quartz cell was used. This particular cell had

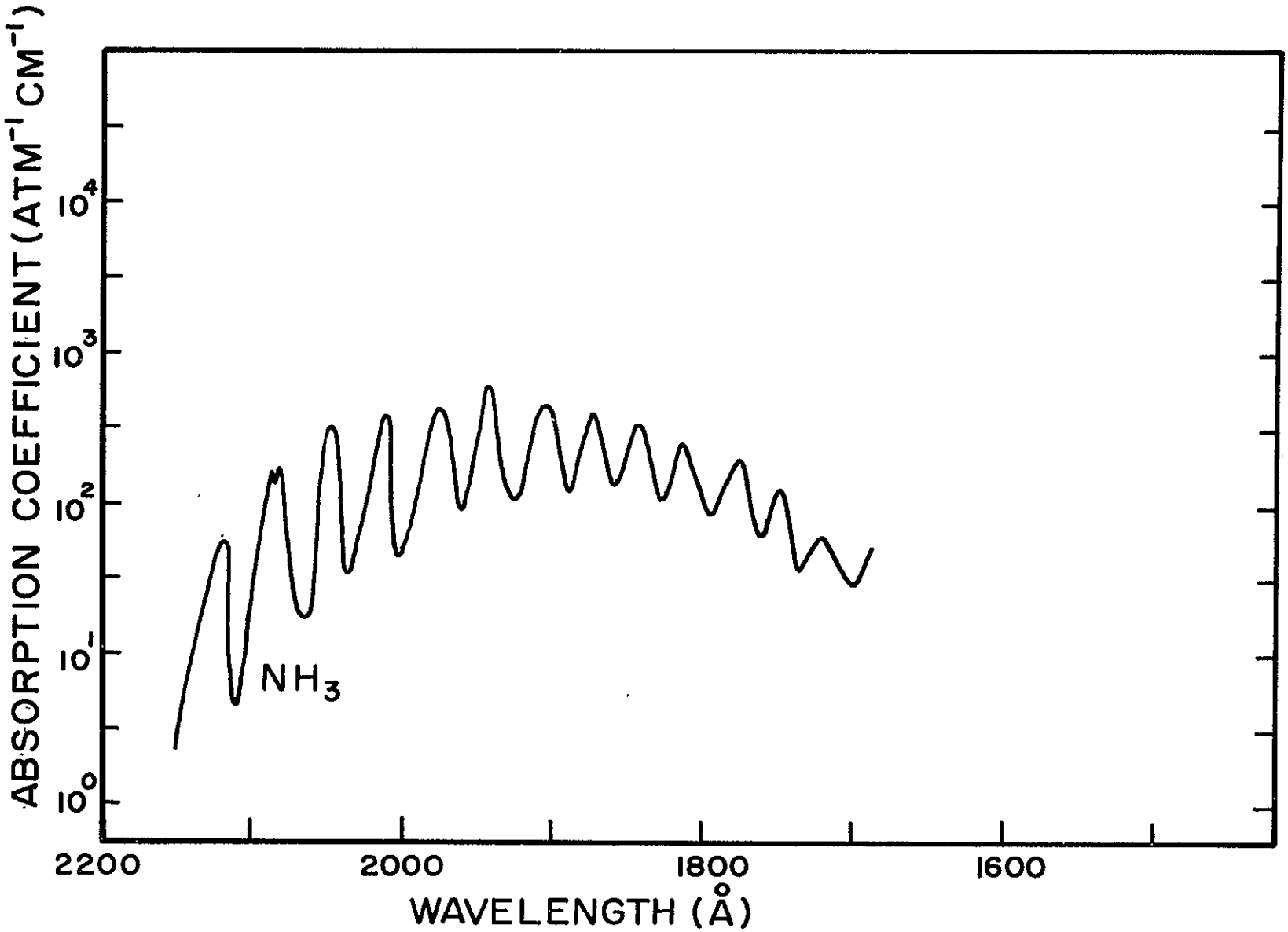

FIGURE 3.1 GASEOUS ABSORPTION COEFFICIENTS BY WAVELENGTH OF NH_3

windows of the same thickness, 3 mm, and grade of quartz as does the photodetachment cell. It volume had been determined by weighing the cell before and after its being filled with distilled water. Each calibration irradiation was made with a pressure of 150 ± 1 Torr argon-ammonia mixture and for a time of 1800 seconds.

Knowing that the volume of the cell is 13.93 cc; that the quantum efficiency for nitrogen production from ammonia is $\Phi = 1/8$; that the time is 1800 seconds; that there are at room temperature 3.3×10^{16} particles per cc at 1 Torr, it is relatively easy to calculate the number of photons of 2062Å light which are reaching the gas per second per lamp window area. The formula follows:

$$\text{photons/sec} = \frac{(\text{pressure } N_2)\ (\text{particles})\ (\text{cell volume})}{(\text{time})\qquad(\text{cc})\quad(\text{quantum efficiency})}$$

The pressure of nitrogen produced in each actinometry run was determined by using the mass spectrometer for analysis. The precision of the measurement was insured by daily calibration of the mass spectrometer for sensitivity to nitrogen. This laboratory's mass spectrometer is calibrated against argon gas. The absolute pressure of argon is measured with a diaphram type micromanometer. The divisions of observed peak height can be measured for a given gas pressure, yielding a ratio of chart divisions per micron of argon gas. The nitrogen is treated similarly, resulting in not only a number of short divisions per micron of nitrogen, but also a number which establishes the mass spectrometer's ability to sense a nitrogen molecule as compared to an argon molecule, that is, the relative sensitivity is determined.

With this in mind, the lamp calibration can be completed using the expanded formula:

$$\frac{\text{Photons}}{\text{sec.}} = \frac{(\text{mole fraction AR})\ (P_o)\ (\text{divisions } N_2)(3.3 \times 10^{16})(13.93)(8)}{(\text{divisions AR})\quad (\text{sensitivity } N_2)\qquad (1800 \text{ sec.})}$$

Thus the number of photons per second per lamp window area can be determined. The number typically for both lamps was in the order of $10^{14} - 10^{15}$ photons per second per lamp window area.

3.4 Calibration for the Hanovia Lamp

The output of the Hanovia mercury discharge lamp at 2537Å was measured using a standard acetone photolysis.[7] A quartz windowed cell of about 50 cubic centimeters was made. This cell was heated by nichrome wire to a temperature of 150° centigrade. The cell was filled with 35 millimeters of acetone vapor. The time of irradiation was 600 seconds. The average of eight irradiations under conditions similar to those used for photodetachment yields on intensity of 1.5×10^{15} photons 2537Å per second. These measurements were made with a 9-54 Corning filter in between the source and the lamp to eliminate the 1849Å radiation of the mercury discharge.

3.5 Lamp Placement

The photodetachment cell has a cylinderical protrusion or cupola into which a lamp can be fit. Initially, this appeared to be a logical implacement. However, as will be discussed in a later section, such an arrangement resulted in an apparent heating effect. The placement of the lamp was finally made at either 40 or 50 millimeters from

the window depending on the distance used in the most recent lamp calibration. By placing the lamp at these distances, the lamp was outside of the protrusion by between 3 and 13 millimeters. The alignment of the lamp to the pyrex surface was achieved by visual method. The lamp was illuminated from behind by an incandescent bulb and the reflection of the flow tube inside the lamp, which is the lamp's longitudinal axis, was aligned with the center of the pyrex surface. Changes purposely made in the perpendicularity of the lamps longitudinal axis with the pyrex surface, at least within the few degrees physically available, did not cause a noticeable effect in the apparent detachment effect.

3.6 Irradiation

The iodine lamp was operated at 210 watts on the power supply wattmeter. At this power level, the lamp's temperature would normally be above room temperature and in fact this was the case. Since the output of the lamp in photons per second was found to vary until it reached its equilibrium temperature, the lamp was always operated for five or more minutes with a physical obstruction between the cell window and itself prior to irradiation. This insured that when the irradiation of the surface was begun, the lamp was at its calibrated intensity. The irradiation was ended by simply turning the power off. The warm-up procedure was not repeated for the next irradiation, however, since the lamp was only off in the order of ten seconds while the physical blockage was replaced, the time to temperature stabilization was only seconds.

3.7 Sampling of Detached Species

Initially, several attempts were made to use a residual gas analyzer as an integral part of the photodetachment system. However, it became apparent that it possessed neither the sensitivity required for analysis nor the capability of maintaining pressures in the order of 10^{-8} Torr.

The method finally used was that of capture by zeolite at liquid nitrogen temperature. The zeolite, now cooled to liquid nitrogen temperature, was exposed to the photodetachment volume while the pyrex surface with condensed gas was irradiated with 2062Å light for 1800 seconds.

Although, the zeolite at liquid nitrogen temperature was known from experiment to adsorb at a rate in excess of 10^{17} particles per second per the five grams used, the physical restriction caused by the MALPHI valve could allow only a passage of in the order of 10^{12} particles per second. Thus, even if there were 10^{14} particles available from detachment, the zeolite could only capture 1% of these. Thus, it was expected that the sample resulting from the zeolite would be small.

To allow for as great a desorption of the collecting zeolite as possible, the sample tube was connected to another evacuated vessel. This vessel was a U-tube connected to another heatable zeolite tube. These two parts allowed isolation of the condensible gas part and the hard gases or uncondensible gases such as nitrogen.

In actual practice, the zeolite collecting tube was heated to 200° centigrade. This was found to be a temperature of very good desorption without effecting the adsorbed gas by dissociation. As this was being done, the desorbed gases were allowed into the liquid nitrogen cooled U-bend volumes and there condensed if condensible. If not condensible, the gases would be readsorbed on the zeolite further on,which was cooled also with liquid nitrogen. After a time of about 10^3 seconds, the separate parts were closed and small amounts, 100 microns, of argon gas were admitted. The two sections were mass analyzed separately. The U-bend was heated with a heat gun just slightly to desorb the gases from its pyrex walls. The zeolite with the non-condensible species was heated to 200 degrees centigrade before being opened to the mass spectrometer.

Part 4

RESULTS AND DISCUSSION

4.1 Thermal Effects Considered

4.1.1 Heating of Cell by Non-Photonic Energy

The most difficult aspect of a photodetachment efficiency, besides maintaining the required high vacuum, is the elimination of thermal effects.

A real thermal effect is seen when the cupola of the photodetachment cell is used as the container of the lamp. It is necessary at this time to take note, that any lower temperature surface within the system tends to have its own adsorbed layer of gas, be it less than or greater than a monolayer in thickness.

In early experiments, it was noted that when the lamp was positioned inside the cupola, an extremely large pressure change was experienced when the lamp was operating. The magnitude of the apparent effect was in the order of 10^{-6} Torr. Since the lamp, when operating, dissipates 200 watts of power, its temperature is 375° Kelvin or more. Thus by radiation it transfers large amounts of heat energy, over a short distance, in addition to its photonic energy. It was assumed then, that part of the pressure change observed was due to a desorption of gaseous molecules from the walls.

A 10^{-6} Torr pressure change in particle density, is, at room temperature, about 10^{10} particles per cubic centimeters. In a volume of 10^{3} cubic centimeters therefore, 10^{13} particles are needed to show a pressure change of this magnitude. Since there are approximately

10^{15} molecules per average monolayer per square centimeter, 10^{13} particles represents one hundredth of a monolayer on one square centimeter or one thousandth of a monolayer on an area of ten square centimeters. By contrast from a steady-state-like calculation or a photodetachment effect, an expected particle density would be 10^{11} particles per thousand cubic centimeters, a mere hundredth of the apparent heating effect.

To test the theory that heating was occurring, the cupola's temperature was raised to 378°K. Thus, accepting the fact that surface coverage by a gas is a function of the reciprocal of temperature, the molecules available for a pressure change by heating would have to then decrease. In turn, the pressure change would be less. This was tried, and indeed, the pressure change magnitude with the lamp on decreased to 10^{-8} Torr.

One further experimental fact had to be reconciled. Even with the temperature of the cupola raised, there was no real constancy to the resulting values. This matter was overcome by moving the lamp to a position outside the cupola. The distances used were four and five centimeters from the quartz window, or 3 and 13 millimeters respectively from the cupola edge. This apparently reduced the heating of the cupola surface by the lamp. A summary of the results from considering the lamp as a source of non-photonic heat appears in Table VI.

4.1.2 Heating of Pyrex Surface by Photon Absorption

It seems reasonable that one might consider some sort of heating effect due to the photons impinging on the pyrex surface. Let

Table VI

Heating by Lamp Radiation

Situation	Magnitude of Effect	Comment
lamp inside cupola cupola not heated	10^{-6} Torr	values reproducible but orders of magnitude too high
lamp inside cupola cupola heated to 378°K	10^{-8} Torr	values not reproducible but right magnitude
lamp outside cupola cupola heated to 378°K	10^{-8} Torr	values reproducible

us assume that there is no gaseous coverage on the pyrex surface. Further, since, as can be seen in Figure 4.1, transmission of light by pyrex glass (Corning 0-53 filter) decreases rapidly with decreasing wavelength, we may assume total absorption of the photons of 2062Å energy although reflection is very possible.

A single photon of 2062Å wavelength has $\frac{1}{2.062 \times 10^{-5}\text{cm}}$ or $4.849 \times 10^{4}\text{cm}^{-1}$ of energy. An entire mole of photons, 6.023×10^{23} in number, would give 138 kilocalories of energy. However $\frac{10^{15}}{6.023 \times 10^{23}}$ moles, a typical photon flux, of 2062Å photons yield 2.3×10^{-4} calories per second. The specific heat of pyrex glass is given as 0.20 calories per degree centigrade per gram.[8] So to raise one gram one degree centigrade, it would take 8.7×10^{2} seconds. However, the pyrex surface itself weighs in the order of (2.6 g/cc x 3.8cc) 9.9 grams. A time period of 8.6×10^{3} seconds would therefore be required to raise the pyrex surface uniformly one degree centigrade. By way of comparison, this time is 2.4 hours, a very long irradiation time. But beyond this, the pyrex surface is directly connected to several kilograms of pyrex glass thus further reducing the heating effect possibility.

It would seem apparent that heating of the pyrex surface by the impinging photons would not be a cause of pressure change even in the smallest measurable amount.

4.1.3 Conduction Effects

The major parameter being measured in this experiment was the change of pressure caused by irradiation of a solid gas by

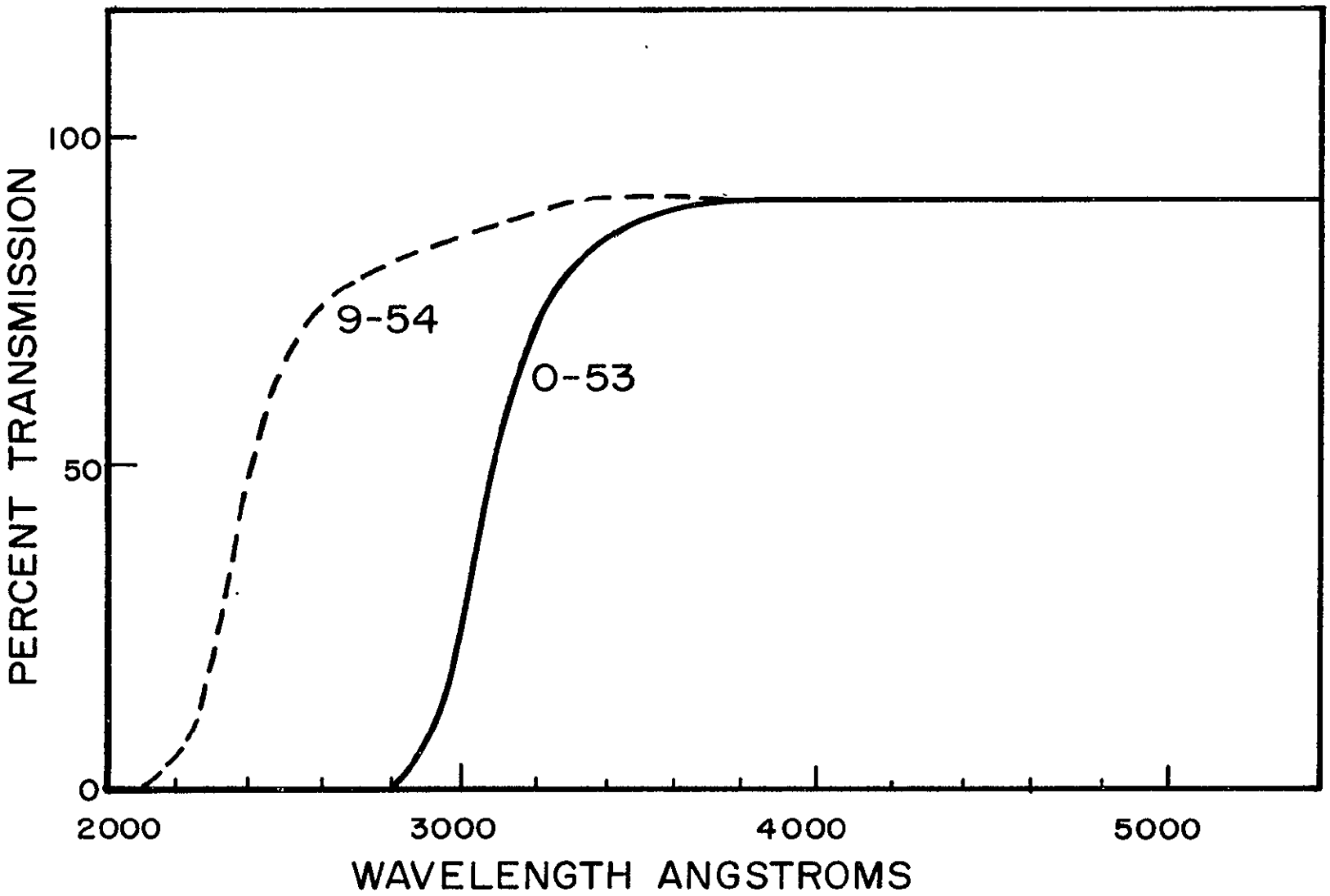

FIGURE 4.1 CORNING FILTER CHARACTER

ultraviolet light. Since pressure also varies with temperature, it is important to maintain a constant temperature of the condensed phase deposited on the cooled pyrex surface throughout any given determination. Heat input via gas conduction or radiation from nearby surfaces would raise the temperature of the deposit. Therefore an estimate was made of the degree of heating as follows.

It is simple enough to calculate the approximate time required for an average molecule to travel from the condensing surface to the quartz window and back again. Because of the closeness of the window, it is not improbable to assume that most of the molecules detached from the pyrex condensing surface do make this trip.

Initially, the molecule was condensed on the pyrex surface. Upon being detached, and assuming it has sufficient energy to escape from the condensing surface the molecule will have a velocity in some random direction perhaps influenced by the lattice of the solid or by the light striking it. The energy distribution of the detached molecules is a difficult problem in itself and will not be further discussed here. Whether or not more than one molecule can be detached under favorable conditions will be discussed in a later section. Nonetheless, the molecule, because of the large mean free path at 10^{-8} Torr, about 10^{6} centimeters, will doubtless strike the walls of the vessel before it encounters another molecule. In so doing, these molecules should, within a single collision with the wall, reach a Maxwell equilibrium with the wall and therefore then possess energy corresponding

to the wall temperature.* After the collision, the molecules will continue their journey at the speed dictated by the wall which was held at a temperature of 378 degrees Kelvin. If the molecules considered are carbon dioxide, after collision with the walls, they will travel at 4.25×10^4 centimeters per second average speed calculated from the formula

$$\overline{\omega} = 1.45 \times 10^4 \sqrt{\frac{T}{M}} \qquad (4.1)$$

where T is the absolute temperature and M is the molecular weight.

If one assumes the distance from the cooled pyrex surface to the window to be one centimeter, a round trip would cover two centimeters distance and on the average, the distance traveled could be as much as four centimeters until the molecule strikes the cooled pyrex surface from which it was detached. If this is so, then the time span from detachment to condensation would be in the order of 10^{-4} seconds.

Noting then that many molecules must return to the cooled pyrex surface in short times, one might question whether or not the returning large number of molecules, with their wall equilibrium temperature, could cause heating of the cooled pyrex surface and therefore a pressure increase due to the temperature increase.

If one calculates the rate of heat exchange by the molecules returning to the cooled pyrex surface, there are two apparent possibilities: first, a heat conductivity type and second, a heat exchange

---

*Polyatomic gaseous molecules, especially the gases investigated, ammonia, carbon dioxide, and nitrous oxide, should be practically equilibrated with the wall temperature after a single collision with it.

by collision of molecules with the cooled surface within a distance λ, the mean free path from the surface.

For the first approach, that of a heat conductivity calculation, two formulae are used. The first equation

$$K = (0.499)\, N\, m\, \bar{\omega}\, \lambda\, C_v = \varepsilon\, \eta\, C_v \qquad (4.2)$$

where K is the heat conductivity constant, N is the number of particles per cubic centimeter, m is the mass per particle in grams, $\bar{\omega}$ is the average speed, λ is the mean free path, C_v is the heat capacity per molecule, ε is a correction factor, and η is the viscosity.

The second equation is

$$Q = K\, A\, \frac{T_2 - T_1}{X}\, t \qquad (4.3)$$

in which Q is the heat transported in calories, A is the area considered, T_2 and T_1 the upper and lower temperatures respectively, X, the distance between surfaces considered and t, the time. The second equation determines the heat flux using the K determined in formula 4.2.

In the first approximation, the value of ε is unity and therefore equation 4.2 becomes $K = \eta C_v$. But, considering only translational energy, Eucken pointed out that for a real gas, the molecules which have a greater velocity have a longer mean free path and therefore transport more heat to a surface. So, the value of heat conductivity from this consideration has to be greater than that assumed by using ε equal to unity.

Since rotational modes are independent of translational modes, the variance of ε from a theoretical value of 2.5 based on the

assumption of toal spherecity and on a r^{-5} repulsion, can be attributed to a summing function. If the total $C_v = C_t + C_r$ then

$$K = (\varepsilon_t \frac{C_t}{C_v} + \varepsilon_r \frac{C_r}{C_v})\eta \qquad (4.4)$$

If $\varepsilon_t = 2.5$ and $\varepsilon_r = 1$ equation 4.4 becomes

$$K = (2.5 \frac{C_t}{C_v} + \frac{C_r}{C_v})\ \eta = \varepsilon\ \eta\ C_v \qquad (4.5)$$

The ε concerned could be calculated from at least two different approxmations, for example that of Eucken and that of Jeans, but instead the experimental values are given for several gases in Table VII. It can be seen that for the gases considered in this investigation, ε is between 1.4 and 1.7.

Table VIII gives heat conductivity coefficients K, for several gases of interest. So, in a carbon dioxide system, at an equilibrium wall temperature of 378 degrees Kelvin using the K value of Table VIII and equation 4.3 and assuming $T_2-T_1 = 300$ degrees, A is equal to 1.27 cm^2, X is 1 centimeter and t is 1 second,

$$Q = \frac{(500 \times 10^{-5})\ (300)\ (1)\ (1.27)}{(1)}$$

$$Q = 1.9 \times 10^{-2} \text{ calories/second}$$

The heat transfer thus calculated is quite large. However, it is doubtful that this quantity of heat is actually transported. The transport of heat energy is most efficient when the mean free path involved in the order of 10^{-5} centimeter. This path length is consistent with one atmosphere pressure. In an actual experiment of the type

Table VII

Values Used for Calculating K
by Equation 4.2

Gas	ε(observed)[9]	ε(Eucken)	C_v x 10^{23}(cal./molecule)
CO_2	1.628	1.57	1.15
N_2O	1.640	1.7	0.89
SO_2	1.601	1.7	1.10
H_2O	1.25	1.7	1.26
NH_3	1.429	1.57	1.20

a) C_v values are average values for the range of interest.

Table VIII

Heat Conductivity Coefficients in 10^{-4} cal. cm^{-1} s^{-1} deg^{-1} at Atmospheric Pressure According to Temperature[10]

	Temperature °C		
Gas	0	20	100
CO_2	0.34	0.38	0.50
N_2O	0.36	-	0.50
NH_3	0.52	-	0.709
H_2O	-	-	0.551

concerned herein, the pressure is about 5×10^{-8} Torr or about 6.6×10^{-11} atmosphere. If the mean free path is 1 centimeter at 10^{-5} atmosphere, then at 10^{-11} atmospheres, the mean free path should be about 10^{6} centimeters. It is this point which makes one question the large heat transport calculated by conductivity equations.

Under the conditions of this investigation, it would be more correct to use a calculation involving the number of molecules returning to the cooled pyrex surface.

$$Q = N C_v (T_2 - T_1) \qquad (4.6)$$

where Q is the heat transported, N is the number of molecules returning to the cooled pyrex surface per second, C_v is the heat capacity of the molecules, and $T_2 - T_1$ the temperature gradient. Assuming 10^{12} particles, a 300 degree temperature gradient, and 6 calories for the heat capacity, Q is calculated to be about 3×10^{-8} calories per second.

It should be noted that the ratio of the calculated collisional heat transfer to the heat conductivity calculated heat transfer is $10^{-8}/10^{-2}$ or 10^{-6}. This ratio is basically correct. Furthermore, the smallness of the collisional heat transfer makes any effect it may have negligible.

4.1.4 Heating by Radiation from the Walls

The walls are very near the cooled pyrex surface on which the sample gas has been deposited. Assuming a black-body like radiation, there could be heating of this solid gas deposit. If one uses the

Stefan-Boltzmann equation

$$E = \sigma T^4 A \qquad (4.7)$$

with $\sigma = 1.38 \times 10^{-12}$ cal deg^{-4} cm^{-1} sec^{-1}, T the temperature of the radiator 378° Kelvin, and A the area one square centimeter, the maximum heat transferred by radiation can be 2.8×10^{-2} calories per second.

It is apparent that there should be a black body like radiation occurring. But, how much pyrex glass radiates like a black body; how much black body radiation does a carbon dioxide or other deposited gas layer absorb; how much of the radiation is just reflected? The calculated value is a maximum and probably the efficiency of heating the deposited gas on the cooled pyrex surface is less.

4.1.5 Cooled Pyrex Surface Temperature

During all the experiments, the dewar was filled with liquid nitrogen. The nitrogen was pumped on to lower its temperature and thereby the temperature of the cooled pyrex surface. At no time was the liquid nitrogen allowed to solidify for then, nitrogen can pull away from the pyrex surface and contact would be lost resulting in a false temperature.

If the maximum radiation of energy from the walls as calculated in section 4.1.4 were to reach the cooled pyrex surface, one can calculate the temperature difference between the two sides of the 3 millimeter thick pyrex plate. The heat conductivity coefficient of pyrex is 24.5×10^{-4} cal cm^{-2} deg^{-1} sec^{-1}. If one uses equation 4.3

$$Q = K A \left(\frac{T_2 - T_1}{X}\right) t$$

where t = 1 sec., A = 1 cm^2 and X = 0.3 cm.

$$Q = \frac{(2.45 \times 10^{-3})\ (\Delta T)}{0.3} = 2.8 \times 10^{-2}$$

$$\Delta T = 3.43 \text{ degrees}$$

This is a maximum value. It should be noted that whatever value this really is, it is approximately constant and does not change with irradiation. Too, the temperature change due to the photon flux of the iodine 2062Å photons would correspond to the heat flux of 2.3×10^{-4} calories as given in section 4.1.2. This would result in a two order of magnitude less change than for the above result, or a change in temperature of only 0.03 degrees.

4.1.6 Relation of Pressure Change to Light Intensity

In order to measure the detachment effect, the most sensitive method available was that of pressure change. Of course, it is assumed that there is a linear correlation between the intensity of incident light and the number of molecules detached.

To prove the relationship of pressure change to light intensity, a series of calibrated copper screens were made. (Figure 4.2 shows the screens). The thought behind their use was that physical blockage of the light is the most reliable technique of reducing the intensity. Table IX gives the ideal values and the results obtained for the four screens when they were placed between the iodine lamp and the scanning monochrometer.

The pressure change due to photodetachment versus light intensity was tested by using the photodetachment cell where a solid

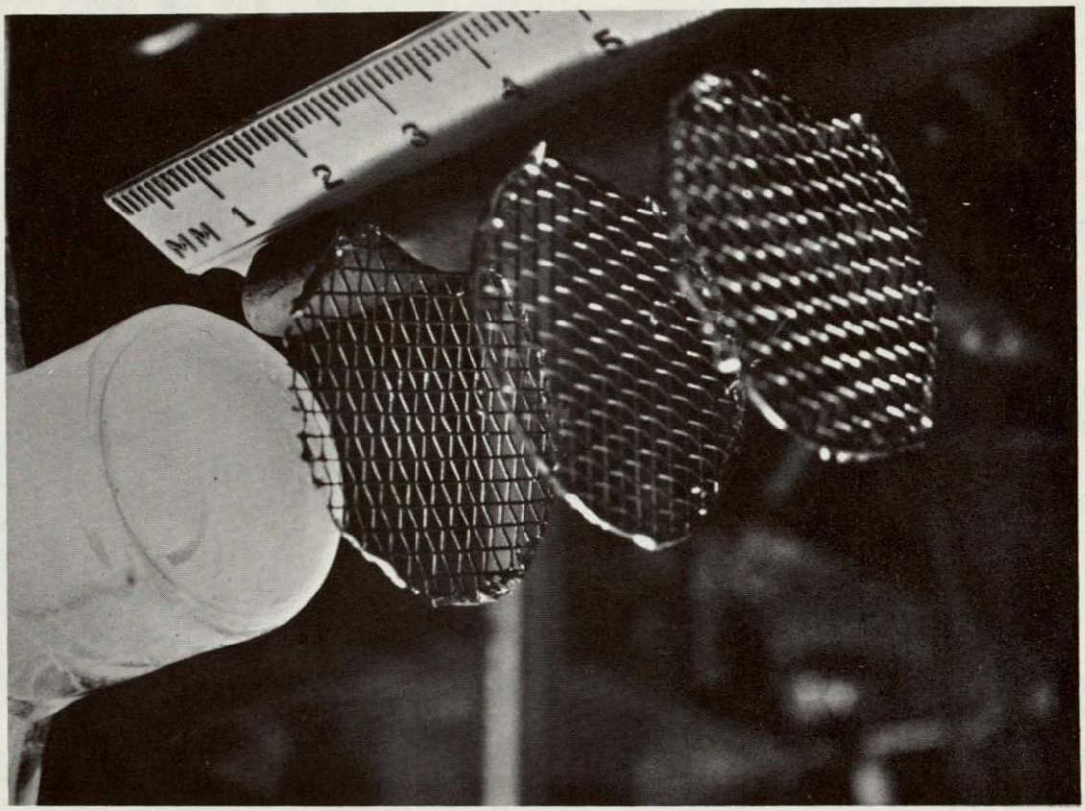

FIGURE 4.2
COPPER SCREENS AND IODINE ARGON LAMP

Table IX

Attenuation of 2062 Å Intensity

Screens	Theoretical	Calculated for Screens	Actual
0	1.000	1.000	1.000
1	0.598	0.675	0.675
2	0.358	0.455	0.45
3	0.214	0.307	0.287
4	0.128	0.207	0.188

carbon dioxide layer was deposited on the cooled pyrex surface. The results of these carbon dioxide experiments are given in Figure 4.3 - 4.6. The error bars shown indicate the standard deviation of the measurements made at each value. The values fall on straight lines through zero showing that as the lamp was used, outside of the cupola and at 210 watts power, the pressure change was due only to the change in light intensity falling on the cold carbon dioxide layer.

4.1.7. Heating by Longer Wavelength Light

If one considers the output of the iodine lamp, even by eye alone much light of the visible spectra is produced. Figure 4.7 gives the line spectra of the lamp. Notably, in the spectra, the 2062Å line stands alone. Any iodine lines to the left of the 2062Å line do not interfer because they are weaker than the persistent 2062Å line and furthermore because they are attenuated by the medium quality quartz used. Figure 4.8 gives the Grotrian energy diagram of iodine. The iodine lamp as developed in this laboratory is practically monochromatic in the shorter wavelengths but there is a not negligible amount of light in the longer wavelengths. Thus, it is apparent from the line spectra that more photons than the number of 2062Å photons are present in the longer wavelengths. But, it can be easily shown that if ten times as many photons in the 3000Å region would strike the carbon dioxide layer as compared to the 2062Å line, the heat effect would only constitue an energy flux of 1.2×10^{-3} calories per second. This is even a decade less than by thermal radiation.

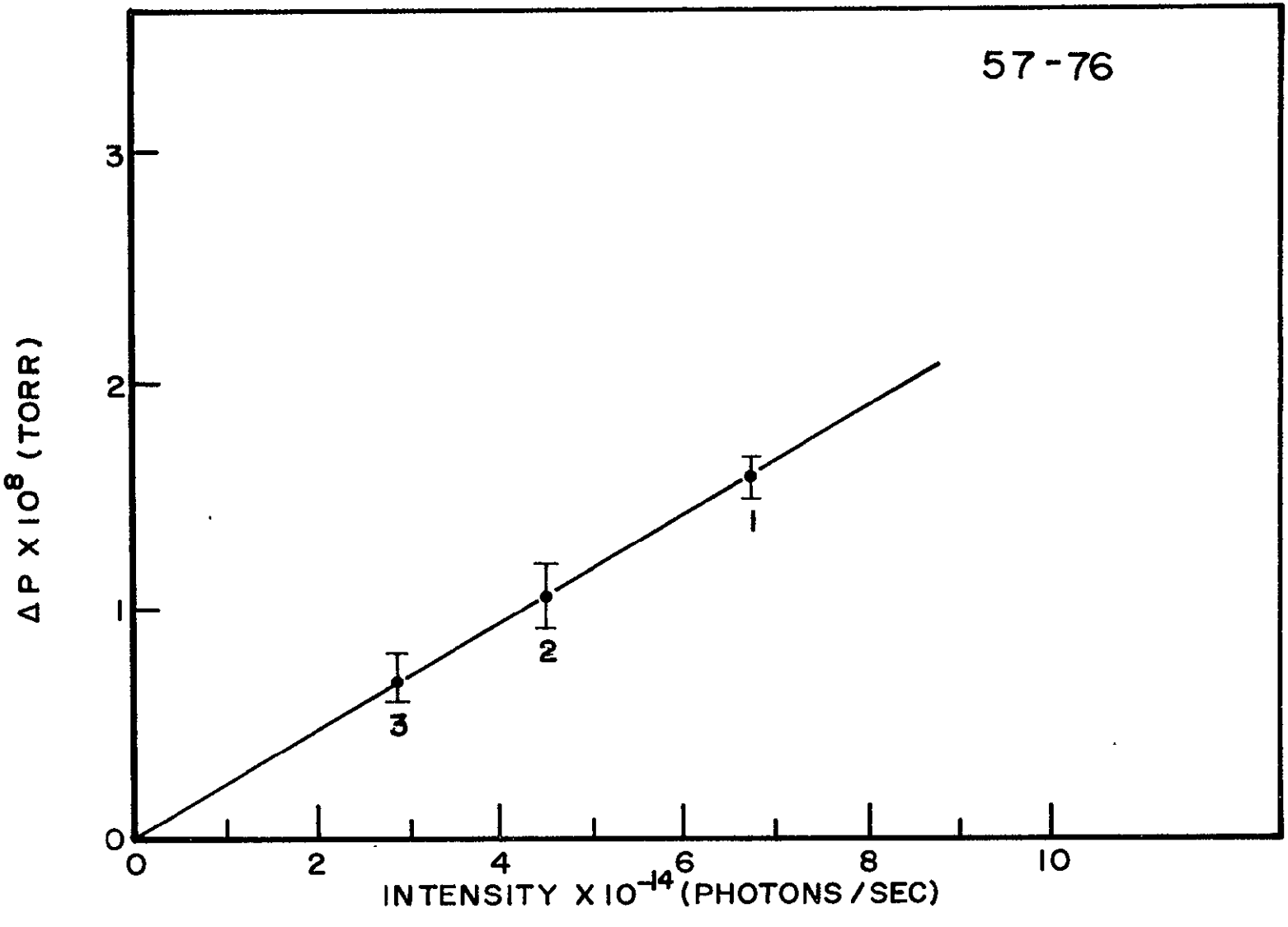

FIGURE 4.3 PRESSURE CHANGE OF DETACHED CO_2 VS. INTENSITY

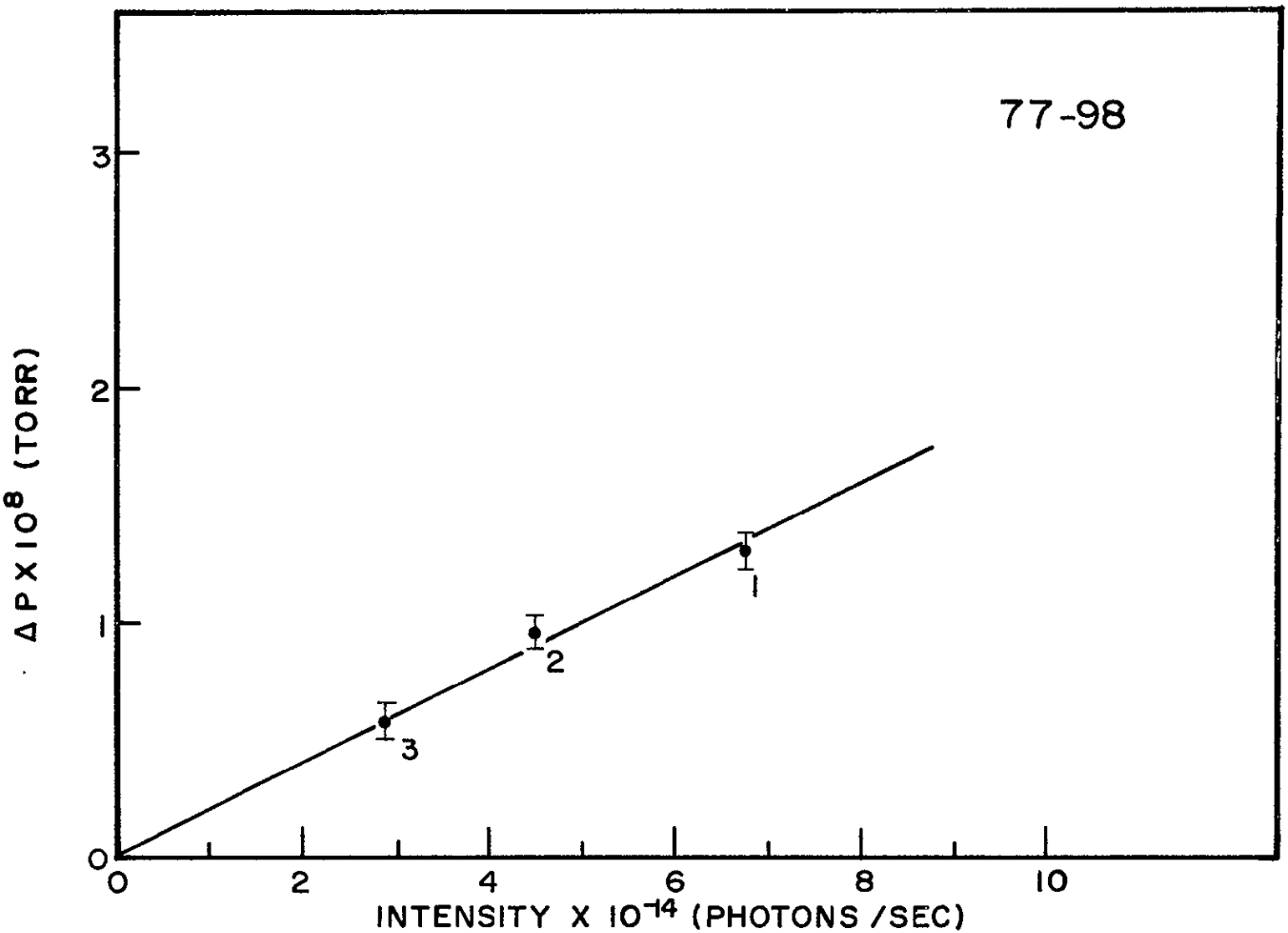

FIGURE 4.4 PRESSURE CHANGE OF DETACHED CO_2 VS. INTENSITY

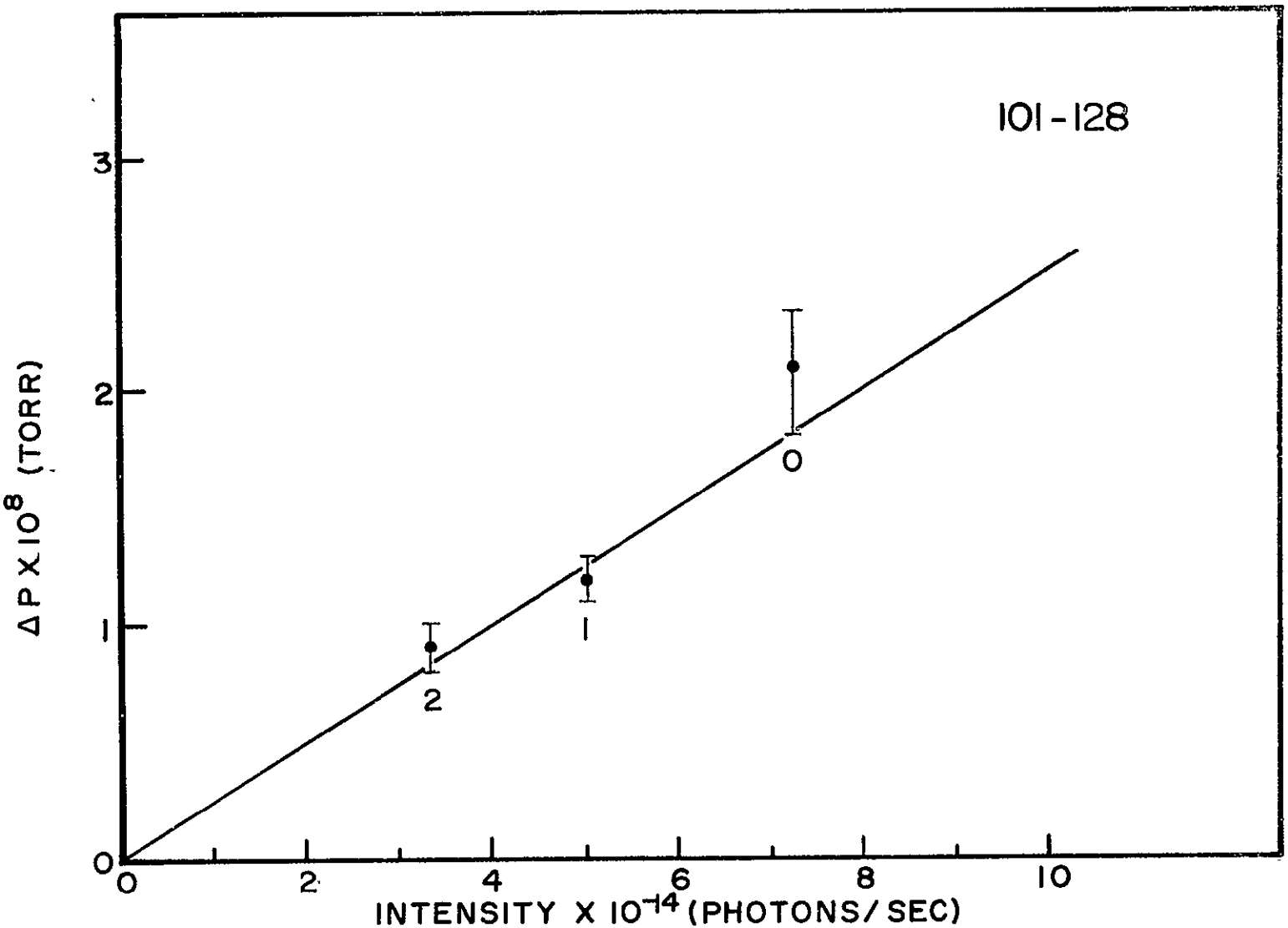

FIGURE 4.5 PRESSURE CHANGE OF DETACHED CO_2 VS. INTENSITY

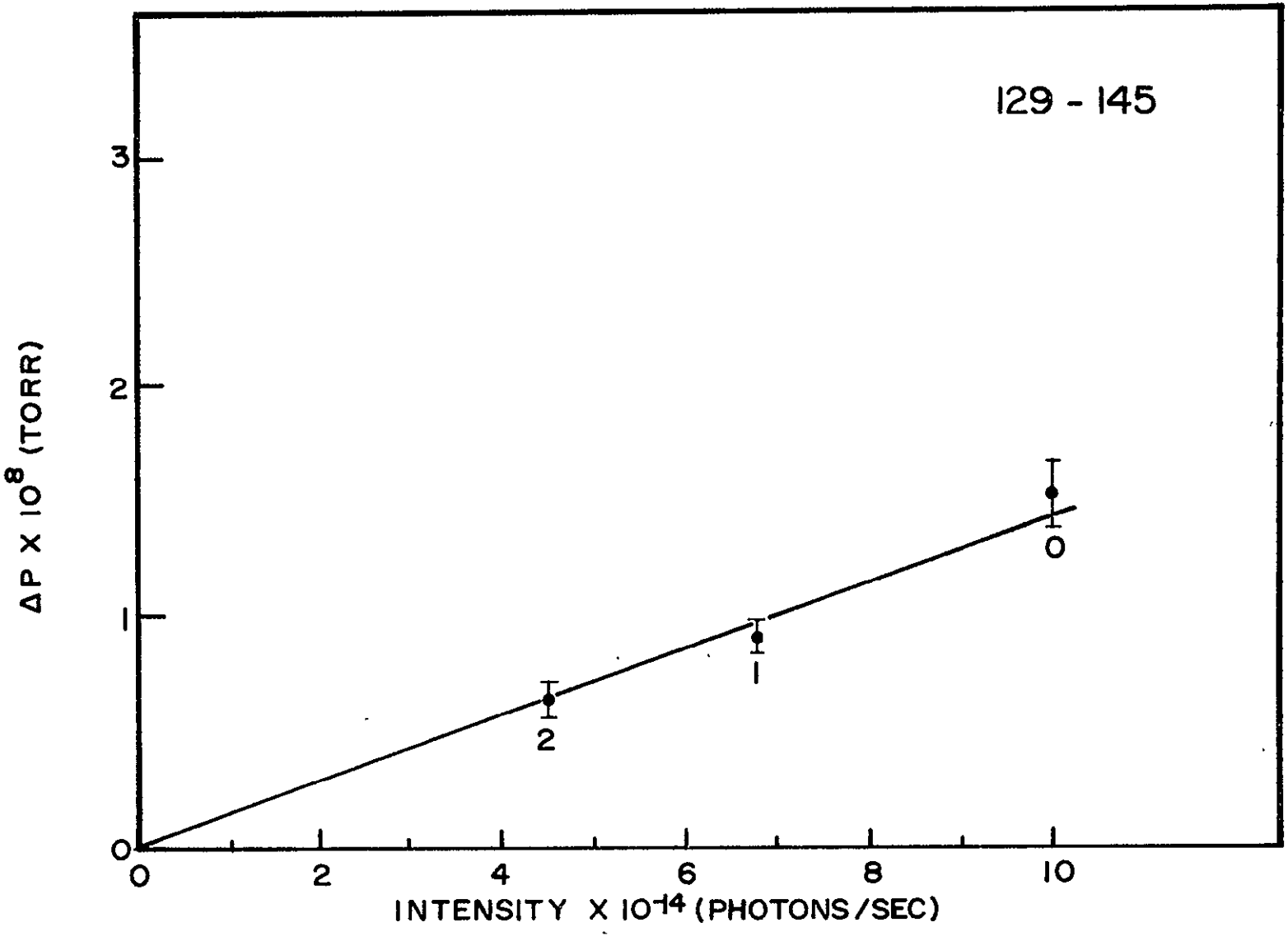

FIGURE 4.6 PRESSURE CHANGE OF DETACHED CO_2 VS. INTENSITY

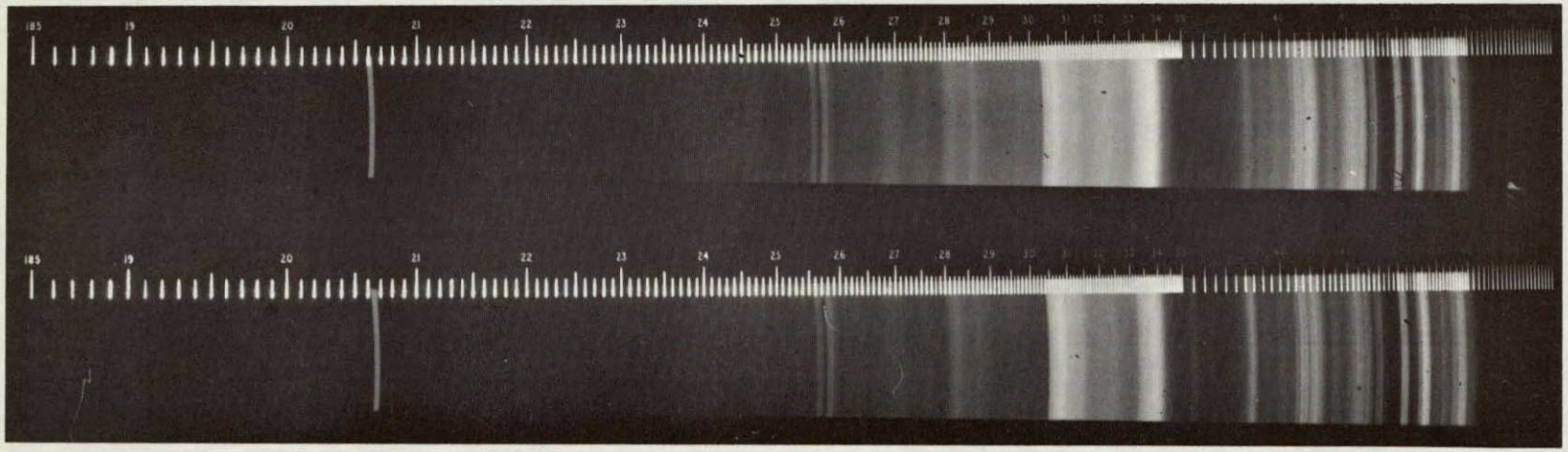

NOT REPRODUCIBLE

FIGURE 4.7 SPECTRA OF IODINE - ARGON LAMP

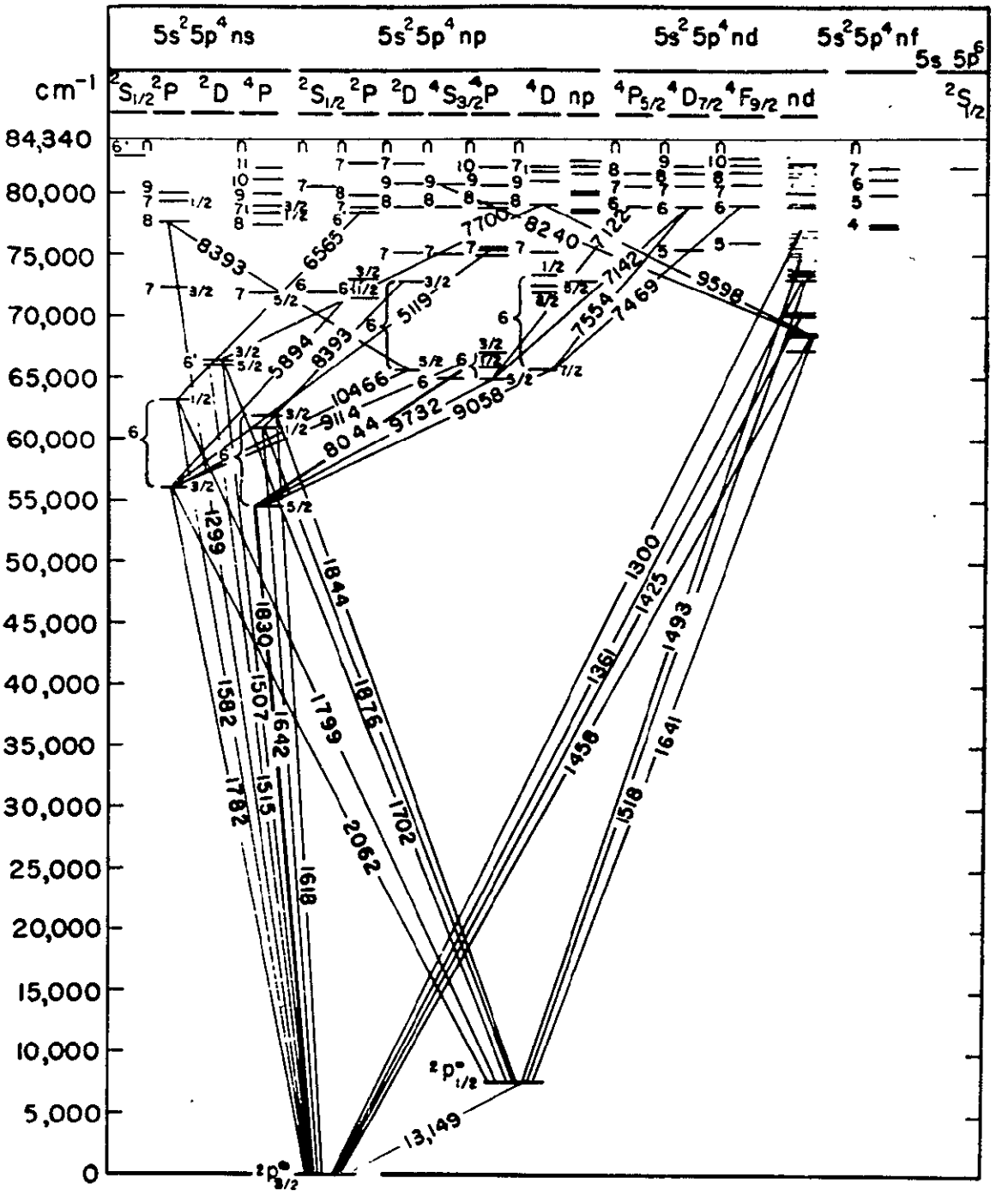

FIGURE 4.8
ENERGY LEVEL DIAGRAM FOR IODINE

However, to test this, glass filters with transmission character as given in Figure 4.1 were used to separate the 2062Å line from the longer wavelength light. A 9-54 filter passes all the longer wavelength light of the iodine lamp and only a small percentage (~5%) of 2062Å light. When the 9-54 filter was used, the pressure increase was only about five percent of the pressure in the photodetachment arrangement when irradiated with the iodine lamp but without the filter. When the 0-53 filter, which does not transmit any light of wavelength less than 2800Å was used, there was no pressure change measurable at all. The results as seen in Table X imply that only the 2062Å line from this particular lamp was effective for photodetachment.

In considering what might have been expected if there was a long wavelength heating effect, graphs of vapor pressure versus temperature change and log vapor pressure versus temperature change were made. The resulting plots for carbon dioxide are given in Figure 4.9 and 4.10. By comparison of the vapor pressure data and the irradiation data, it can readily be seen that at the temperatures of the investigation, 72°K and less, the vapor pressure change for a temperature change of one degree is in the order of 10^{-9} Torr whereas the photodetachment effect gives rise to a change of 10^{-8} Torr. Ammonia has no vapor pressure whatever ($<10^{-11}$Torr) at these temperatures, and the vapor pressure of nitrous oxide, compared to carbon dioxide, is about a decade higher, but still does not interfer.

Table X

Results of Filter Studies of Iodine Argon Lamp by Individual Gas

Gas	Pressure Change x 10^8 (Torr) Valves Closed 0-53	9-54
CO_2	0	0.15 ± 0.02
NH_3	0	<0.1
N_2O	0	<0.1

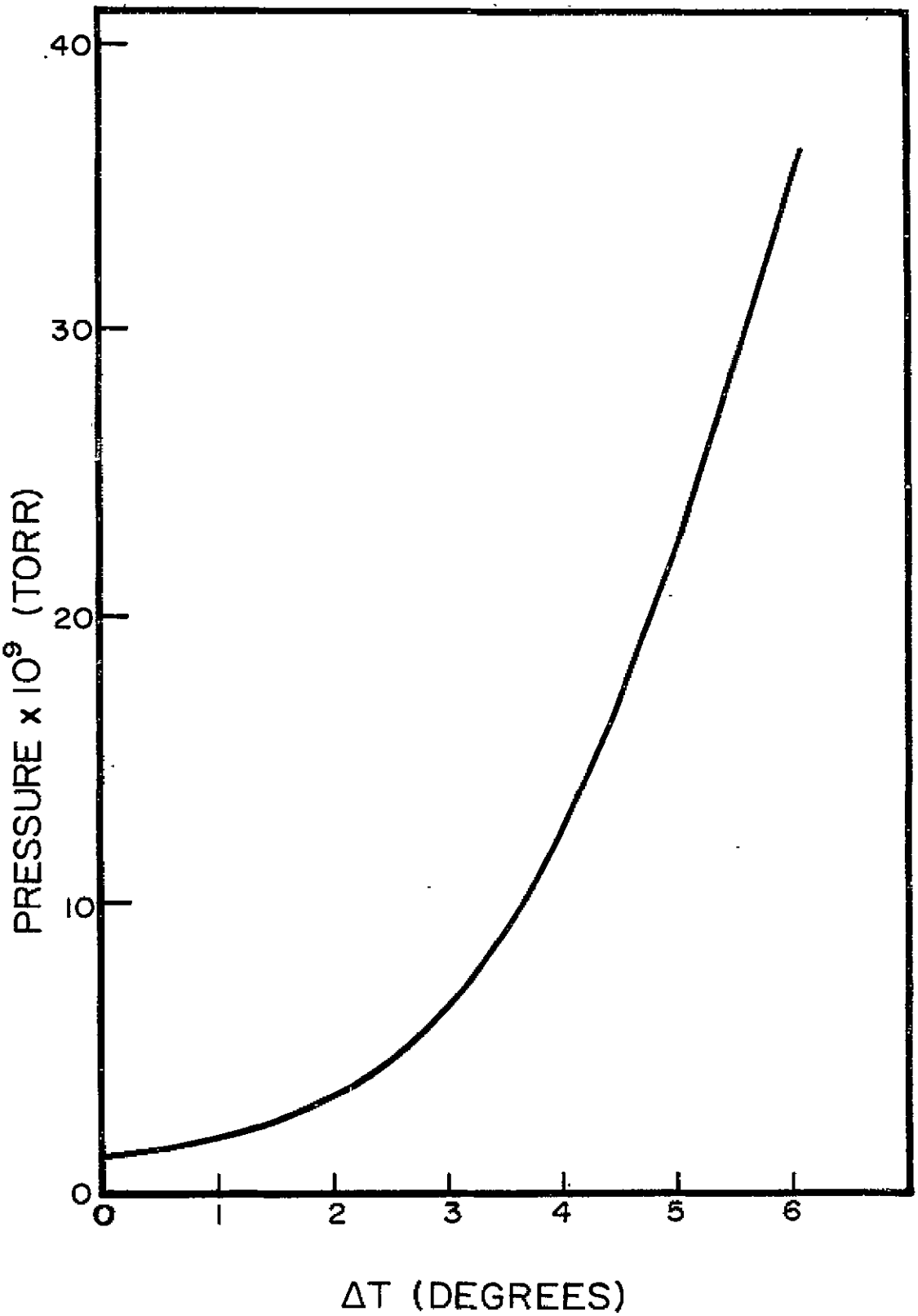

FIGURE 4.9 VAPOR PRESSURE VS. TEMPERATURE CHANGE FOR CO_2

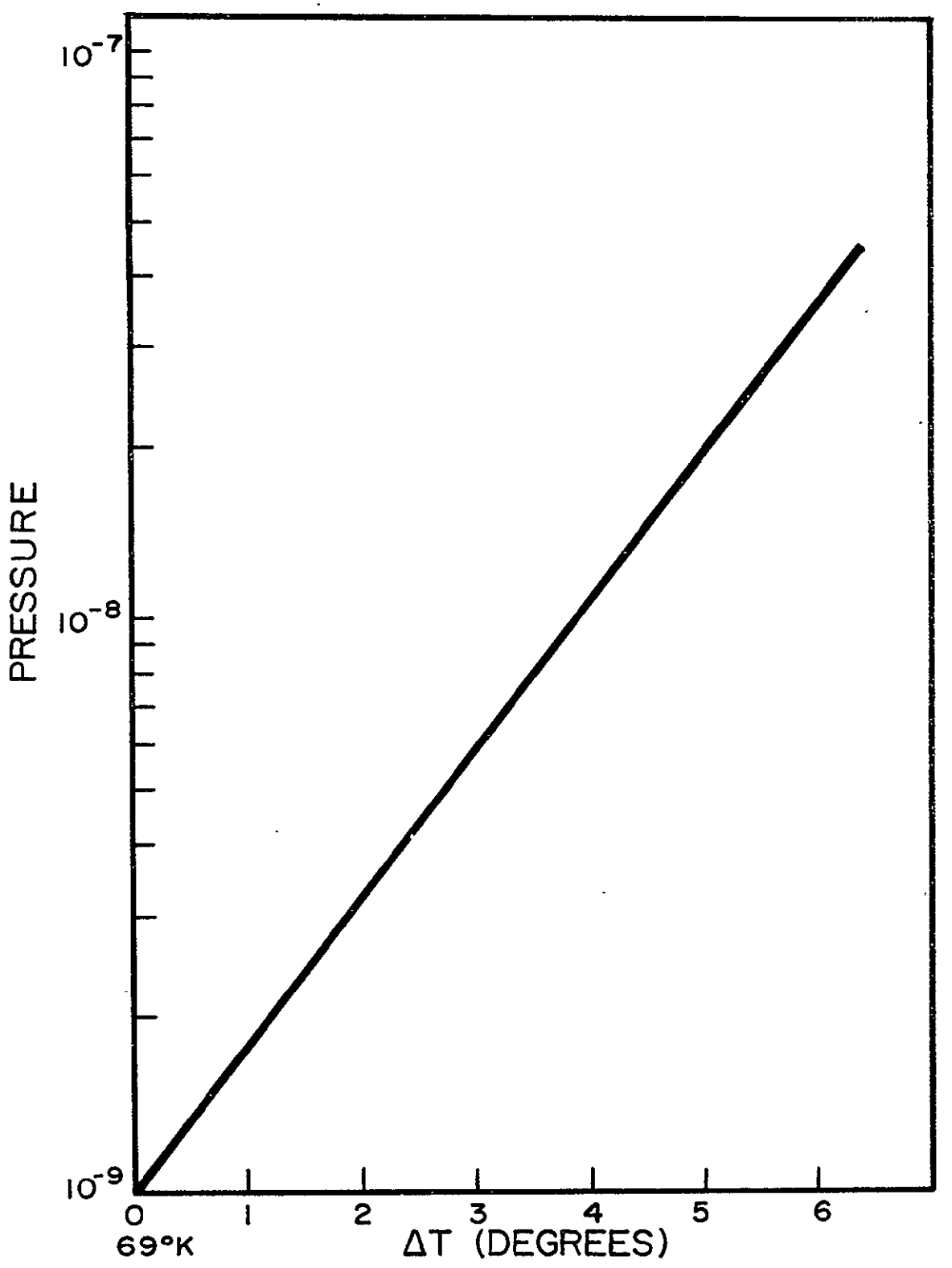

FIGURE 4.10 LOG VAPOR PRESSURE CO_2 VS. TEMPERATURE CHANGE.

4.2 Absorption of Photons

A prerequisite for an observable photodetachment effect is that absorption of the incident light occurs in the upper layers of the substance. The photodetachment effect is dependent upon our ability to establish experimental conditions under which the light is absorbed so that the photodetachment effect occurs and can be measured.

It is known that the gases involved here, carbon dioxide, ammonia, and nitrous oxide do absorb light in the ultraviolet. However, only ammonia has an appreciable absorption coefficient at 2062Å. The absorption coefficients of carbon dioxide and nitrous oxide are very minor and by 2537Å all three gases are, for all practical purposes of this investigation, completely transparent. Figure 4.11 and 4.12 give the absorption coefficients of these three gases, as well as that of water, as presented by various authors.[11-23] Because of the small absorption coefficients in the gas phase, and the very low pressure and short distance from window to cooled pyrex surface, the photodecomposition of these constituents in the gas phase is entirely negligible.

The solid state of these substances presents still another situation. Figure 4.13 gives the absorption coefficients with wavelength for the solid phase ammonia, water and nitrous oxide.[24-28] It is interesting to note that for ammonia, the absorption coefficient remains in the same order of magnitude for 2062Å light and loses its structuring. For wavelengths less than 1950Å, however, its absorption coefficient both increases in value and loses its structuring also. (see Figure 4.13). The absorption coefficient for water is noticeably

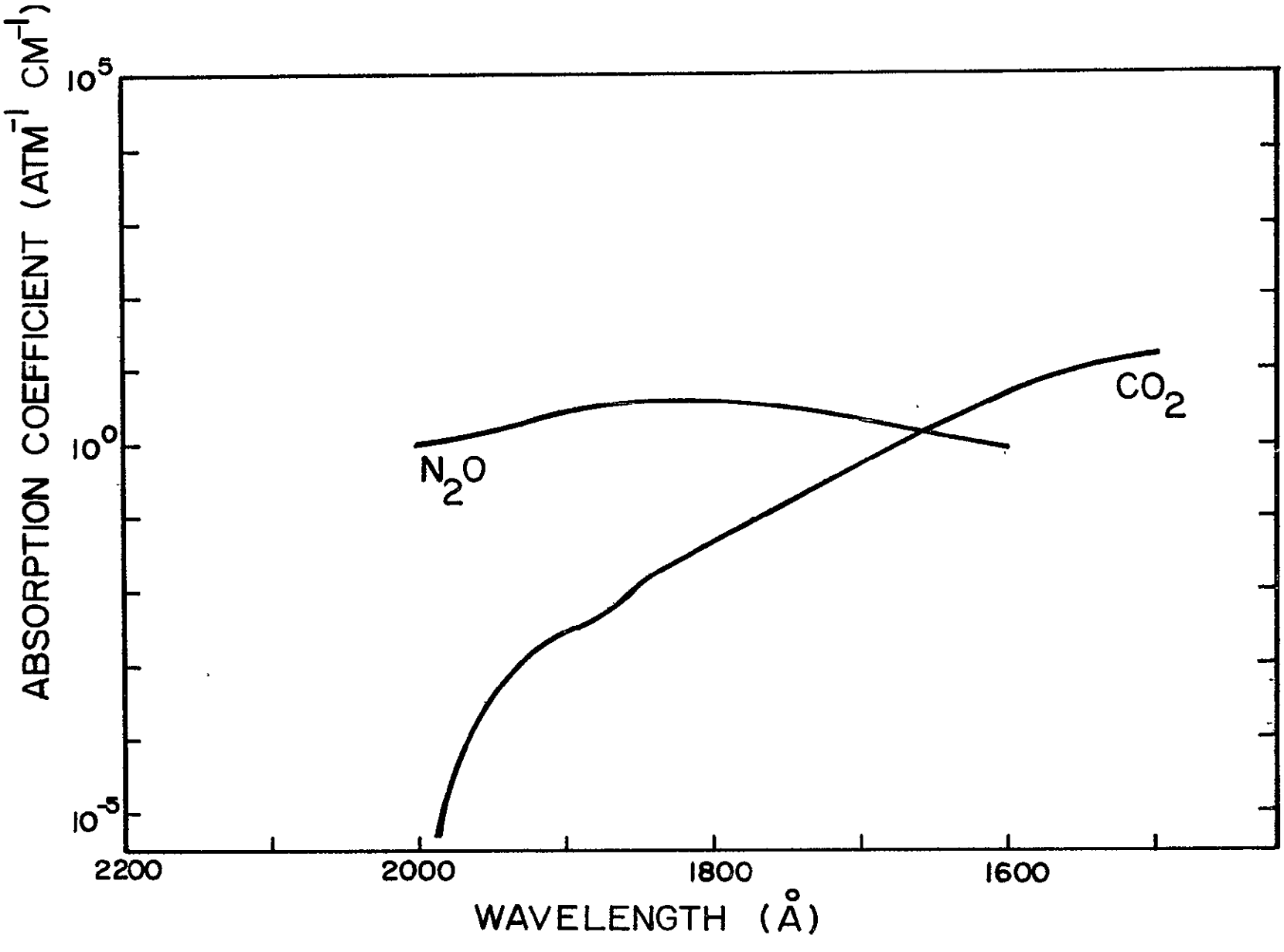

FIGURE 4.11 GASEOUS ABSORPTION COEFFICIENTS BY WAVELENGTH OF CO_2 AND N_2O

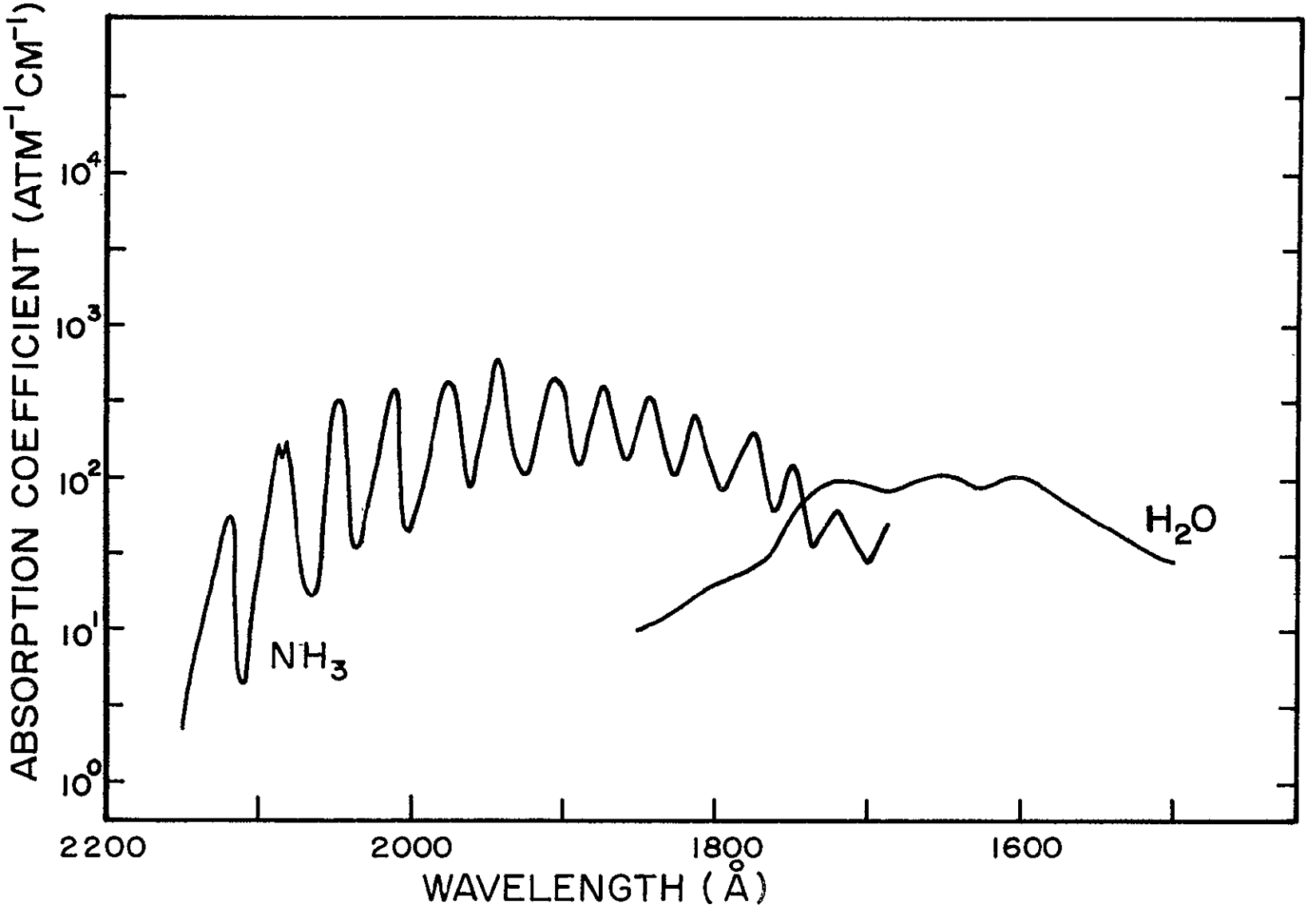

FIGURE 4.12 GASEOUS ABSORPTION COEFFICIENTS BY WAVELENGTH OF NH_3 AND H_2O

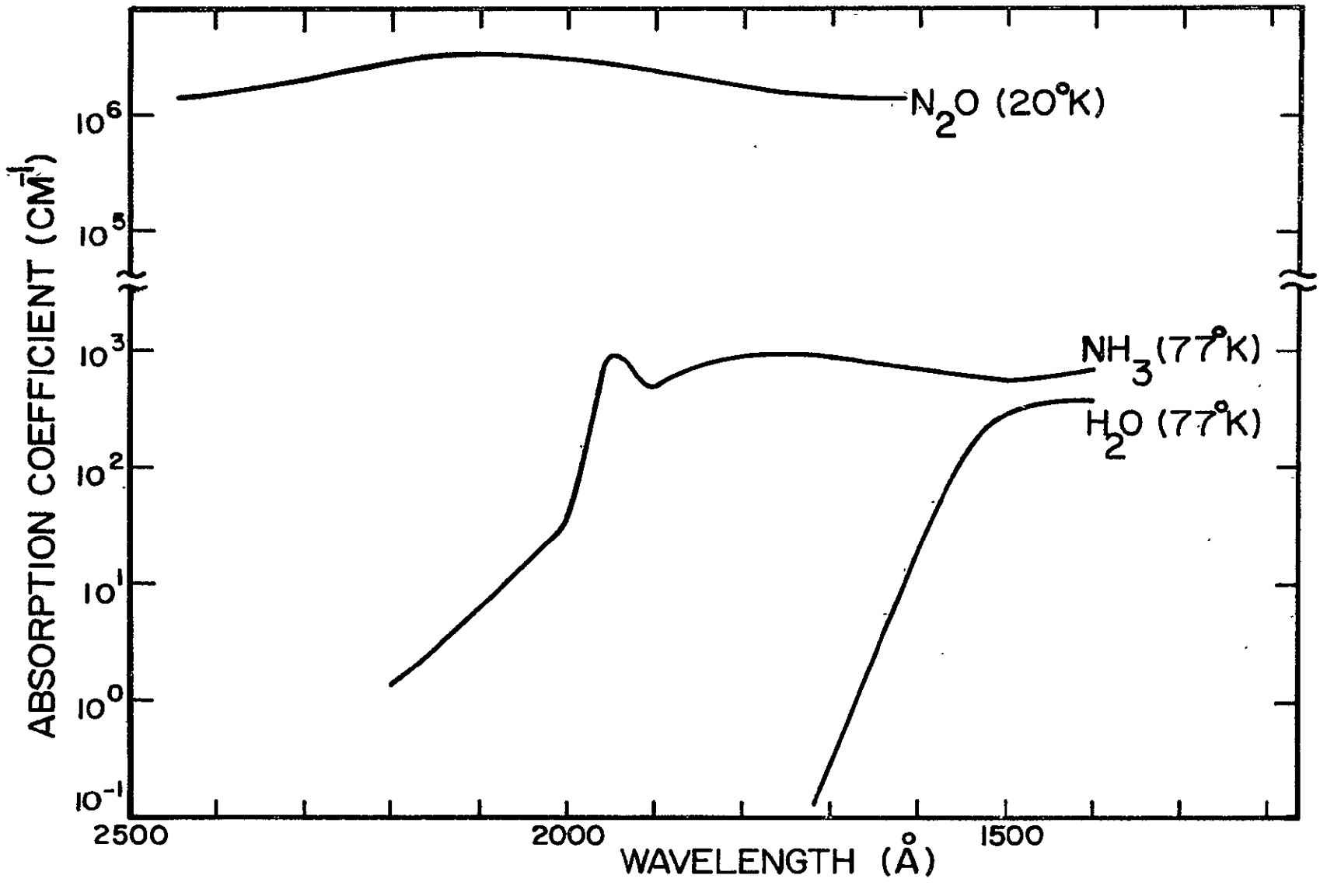

FIGURE 4.13 ABSORPTION COEFFICIENTS OF SOLID GASES AS A FUNCTION OF WAVELENGTH

displaced to shorter wavelength by about a hundred angstroms. The nitrous oxide absorption coefficient in the gas phase shows a value of 4 atm^{-1} cm^{-1} at about 1850Å, whereas the solid shows a spectacularly large absorption coefficient of 10^6 cm^{-1} at a maximum shifted to the longer wavelength 2100Å. It is worthy of note also, that for all the solid gases investigated, the absorption coefficient is greater at 2062Å than at 2537Å.

Absorption coefficients for solid or liquid carbon dioxide could not be found in the literature. Several attempts however, were made by us using both an existing dry box isolation method and an existing all quartz cell with evacuated insulation chamber to try to measure the absorption coefficient of carbon dioxide, but with no result. Obviously such results are not obtainable by such shot gun experiments. Noting however that carbon dioxide and nitrous oxide are iso-electronic and are quite closely related in Van der Waals, configurational, and kinetic behavior, one is tempted to correlate the two to some degree in solid state absorption coefficients. If one notes that the maximum of the 1400Å to 2800Å range for solid nitrous oxide is shifted by about 8000 wavenumbers, and its specific absorption coefficient increased by a factor of 10^3 at 2062Å, one need only assume that carbon dioxide may follow a similar pattern both in respect to wavelength maximum shift and absorption coefficient. Using values similar to the nitrous oxide shift, the 60,000 cm^{-1} intense absorption of carbon dioxide could conceivably be shifted to 52,000 cm^{-1}. Such an absorption could carry over to 2062Å with a high value for the

absorption coefficient. Although the absorption coefficient for solid carbon dioxide, at this writing is speculative, the very fact that photodetachment phenomena effects do occur lend credence to this assumption.

4.3 Pressure Change by Photodetachment

Each of the gases examined, ammonia, carbon dioxide, and nitrous oxide under the proper conditions gave a photodetachment effect. Without taking into account any dissociation which may occur, the change in pressure due to irradiation was recorded. Table XI gives the results listed by gas and by the valving of the photodetachment system. The headings "valves open" and "valves closed" refer to the position of the MALPHI valves. In the "open" condition the main pump is open to the photodetachment volume. In the "closed" condition, the photodetachment volume is isolated.

4.3.1 Pre-irradiation Pressures

As given in Table XII, there were, under the experimental conditions, background pressures in the order of 10^{-8} Torr for all the gases investigated, even though the temperature of the cooled pyrex surface corresponded to a lower vapor pressure of the solid deposit of gas. Immediately, one might assume an air leak. However, if this were the case, as pumping on the photodetachment cell was stopped, the pressure would increase, and continue to increase linearly with time. Likewise, if some substance were assumed to be decomposing within the system, the pressure would rise as the pumping was stopped and the

Table XI

Pressure Change with Valves Open and Valves Closed for 2062Å Line

Gas	Valves Open $\Delta p \times 10^8$	Valves Closed $\Delta p \times 10^8$
CO_2	0.66 ± 0.05*	2.16 ± 0.02
NH_3	0.63 ± 0.05	1.74 ± 0.02
N_2O	0.87 ± 0.05	2.14 ± 0.02

Values given are average for sets of experiments run on the same day.

*These limits of error are somewhat arbitrarily derived from the combination of errors in a single measurement and the reproducibility of the experiments.

Table XII

Pre-Irradiation Pressures for Various Gases as Function of the Valve Position at Approximately 72°K

Gas	Valves Open $p \times 10^8$	Valves Closed $p \times 10^8$
CO_2	2.5 ± 0.05	5.0 ± 0.02
NH_3	1.8 ± 0.05	4.5 ± 0.02
N_2O	3.0 ± 0.05	5.8 ± 0.02

pressure would increase linearly with time. However, when the pumping is stopped in the photodetachment system, immediately (within two or three seconds) the pressure increases to its maximum non-irradiated value and does not further increase with time. These background pressures are reproducible as pumping is started and stopped with the opening and closing of the MALPHI valves.

As discussed in section 4.1.5, one might assume that the background is at least partially due to the difference in temperature between what is measured by the vapor pressure of the liquid nitrogen and the real temperature which exists on the side of the cooled pyrex surface where the solid gas is deposited. This does not appear to be the case since vapor pressure data for the gases used do not give pressure values which correspond to the pre-irradiation pressures even if the maximum temperature difference calculated in section 4.1.5 is allowed.

Another explanation however has real value. If one recalls the positioning of the collar around the cooled pyrex surface, one will also recall that it sticks out into the volume toward the heated walls. Thus, even though it is physically a continuous piece of glass with the cooled pyrex surface, it may well have a temperature higher then the cooled pyrex surface. If the fact that solid gases have been known to migrate along a surface, is coupled with the assumption of a slightly higher temperature of the collar, it is not difficult to imagine that some of the solid gas deposit does migrate to the slightly warmer collar, where it assumes the vapor pressure appropriate for its higher

temperature. As the molecules are freed from the deposit on the collar edge near the cooled pyrex surface, they of course start a journey which will take them back to the cooled pyrex surface. However, before they are recondensed they will contribute to a background pressure. The reasonableness of this discussion becomes apparent, when one considers that the background pressure of 5×10^{-8} Torr in a volume of 10^3 cubic centimeters accounts for approximately 10^{12} particles and at 10^{15} particles per monolayer per centimeter square, this is only a monolayer on an area of 10^{-3} square centimeters. It is easily imagined that such small quantities of solid deposited gases do migrate. Furthermore, the reproducible different backgrounds for each of the different gases makes this reasoning all the more plausible because the backgrounds appear to be characteristic of the individual gas concerned.

4.4 Steady State Consideration

The experiments of this investigation were run based on the existence of a steady state as expressed in equation 4.8.

$$\Phi \zeta K = 1/4 \, n \, \bar{\omega} \, A \, \Gamma \qquad (4.8)$$

where Φ is the number of light quanta passing through the quartz window; ζ is the efficiency of photodetachment; K is the fraction of the light which falls on the deposited gas on the cooled pyrex surface; n is the particle density in molecules per cubic centimeter; $\bar{\omega}$ is the average velocity of the molecules in equilibrium with the walls of the vessel which were held at 378 degrees Kelvin; A is the area of the cooled pyrex surface in square centimeters and Γ is the efficiency of recondensation.

Equation 4.8 assumes that the number of molecules detached per second according to the left half of the equation equals the number of molecules recondensed per second according to the right half of the equation.

4.4.1 The Efficiency of Condensation on the Cooled Pyrex Surface

Table XI lists the photodetachment pressure changes according to the valve position. One may notice that for carbon dioxide, the "closed valve" value is three times as high as the "open valve" value. This would seem to indicate that there are a substantial number of molecules which can be pumped away. This leads in turn to the thought that recondensation of the detached molecules is not as efficient as might be expected. A collaborating fact, to the above, is that when the cell is filled with a gas and the conditions are made for condensation on the cooled pyrex surface, even after a day, the system has not come to the pressure equilibrium in which all the molecules have condensed on the surface of lowest temperature. All the gases used for the photodetachment, after a day, did reach a 10^{-8} Torr pressure which was practically the same.

A simple comparison of pumping ability of the condensing window and the MALPHI valves and tube can be made. The cooled pyrex surface should pump like an orifice. So, its conductance should be

$$F = 1/4\ \bar{\omega}\ A \qquad (4.9)$$

where F is the conductance; $\bar{\omega}$ is the average velocity; and A is the area in square centimeters. The MALPHI valves, of which there are two in series with 100 centimeters of 1 centimeter radius tubing will have a

conductance related to all three. Each MALPHI valve alone conducts by equation 4.9. The tube follows equation 4.10 as an approximation.[29, 30]

$$F = 100 \frac{r^3}{L} \qquad (4.10)$$

where F is the conductance; r is the radius; and L is the length of the tube. The conductance for the cooled pyrex surface, using an area of one square centimeter and a velocity of 4.25×10^4 centimeters per second is 10.6 liters per second. The series value for the MALPHI valves and the tube using a radius of 0.25 centimeter for the MALPHI valves, a radius of 1.0 centimeters for the tubing and a length of tubing equal to 100 centimeters is

$$F = \frac{1}{\frac{1}{2.2} + \frac{1}{2.2} + 1}$$

$$F = 0.524 \text{ liters per second.}$$

Comparison of the two values indicates that if the cooled pyrex surface condensed each particle which strikes it, it should be 10/0.524 or 19 times as efficient as the pump. Experiment however shows that the pump is three times as efficient as the cooled pyrex surface. Thus overall, the cooled pyrex window has an approximate recondensation efficiency of 1/57. A useful value should be about 1/40.

There are a series of possibilities which might be used to evaluate these results. A very detailed calculation of the resistence of the system and its relaxation time both with the system "open" and "closed" can be made. Sophisticated assumptions may be made to correlate the results. But after all of these, the answer should fall in

the same value region and nothing will have been added to the basic understanding of the problem. We will have only succeeded in making the problem still more complicated.

The photodetachment system has been calibrated for its pumping character. We added, for example, nitrogen gas and recorded the pressure change with time. This calibration allows at least an estimate of the amount of photodetached species one can expect to be pumped away during an irradiation of the deposited gas with ultraviolet light if the valves are "open".

The reason why condensation is not fast is a problem in itself and may very well be due to the fact that the surface which the deposited gas presents to returning molecules is covered with dendrite-like structures where it may take the returning molecule a substantial time to find its place in the lattice. This is indeed a fascinating problem, but it is not the purpose of this paper.

4.5 Photodetachment Efficiency

The results of the calculation of photodetachment efficiency for the three gases examined are given in Table XIII. Γ, the recondensation efficiency was assumed to be 0.025 for this system.

The calculation accepts the fact that no large amounts of photodissociation of molecules occurs either in the solid or gas phase.

Absorption in the gas phase is given by the well known formula

$$I = I_o (1 - e^{-\alpha x P/P_o})$$

Table XIII

Efficiencies of Molecular Photodetachment in Units of Molecules/Photon

	ε(molecules/photon)
CO_2	7.7×10^{-4}
N_2O	7.5×10^{-4}
NH_3	6.0×10^{-4}

Calculated by equation 4.8

In the case of ammonia which has an absorption coefficient of about 30 atm^{-1} cm^{-1}, the gas phase absorption is negligible. By calculation, there are only 10^6 absorption occurrences per second, so in 10^3 seconds there are only 10^9 such occurrences. The other gases, carbon dioxide and nitrous oxide have still smaller absorption coefficients and so the dissociation extremely minor.

Ammonia can be dissociated by 2062Å light. However, since the pressure due to photodetachment is reversible when the irradiation is stopped, it becomes apparent that there is no large amount of dissociation products in the gas phase which could interfer with the pure detachment effect.

If dissociation were to occur in the deeper levels of the deposited solid ammonia, the products may be unable to diffuse to the surface and go into the gas phase but could easily remain occluded.

In the case of carbon dioxide, concerning the possibility of dissociation, the following point must be considered. The reaction $CO_2 \rightarrow CO + O$ requires 128 Kilocalories, and the energy of the 2062Å line is 138 Kilocalories. Therefore, any absorbed light quanta has sufficient energy to dissociate a carbon dioxide molecule. However, if dissociation would occur, CO_2 and O-atom must react to form $CO + O_2$, but, this is 9 Kilocalories endothermic. Thus, it is very unlikely that this reaction should be a primary reaction, especially if one considers that in the gas phase carbon dioxide only absorbs reasonably and becomes dissociated where the carbond dioxide molecule is dissociated into a carbon monoxide ground state and an $O\ ^1D$.

It must also be realized that if the energy is only sufficient to dissociate a molecule, due to the socalled "cage effect", the products will recombine. The "cage effect" since its discovery by E. Warbury in 1918 has been discussed by many other authors. The idea is always that if only enough energy or a little more than required for dissociation is available, the fragments will remain very near and will very likely recombine at once.

A similar consideration can be applied to the nitrous oxide. However, there is one big difference. Whereas the binding energy for CO + O is 128 Kilocalories. It is also well known that the reformation of N_2O by the recombination of N_2 + O requires a heat of activation of 10-12 Kilocalories. This would inhibit the reaction at the low temperatures of the solid phase.

A long discussion might be made considering why or why not a photodissociation should or should not occur, however, in this case the experimental evidence is that during the irradiation process, no fragments of N_2O such as N_2, O-atoms, or O_2 are measured.

Figure 4.14 gives a tracing of an actual carbon dioxide scan. Its extreme symmetry indicates the lack of photodissociation.

There is also a limit to the occurrence of photodetachment. Photodetachment cannot occur when, if for example, the quanta absorption occurs 10^2 monolayers deep in the solid matrix. The energy may be used up in dissociation or in other modes of energy and no particle would be able to penetrate the 10^2 layers and escape to the gas phase. However, the effect of upper layer absorption of quanta in the solid is

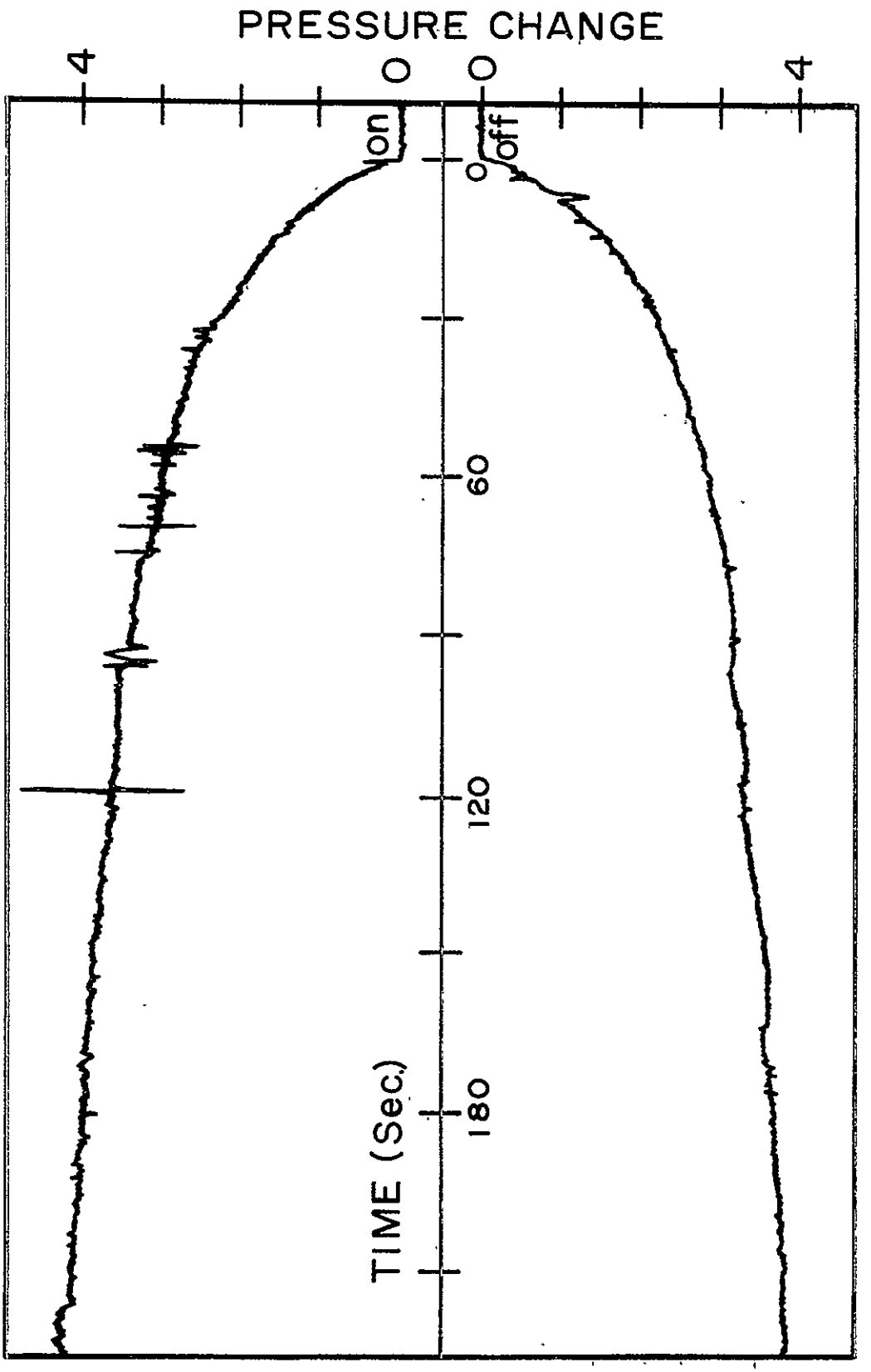

FIGURE 4.14 SYMMETRY OF CO_2 PRESSURE CHANGE

different. Since the heats of sublimation per mole of the substances considered are in the order of 5-6 Kilocalories, and the 2062Å line is equivalent to 138 Kilocalories the energy would be sufficient to evaporate large amounts of molecules. Obviously, this does not seem to occur.

Therefore, as has been seen, a high absorption coefficient is a prerequisite for an observable photodetachment effect. If, for example, the absorption coefficient is 10^6 and one molecule has a diameter of approximately 3×10^{-8} centimeter, then in the first layer, 3 percent of the total energy is adsorbed. If the attenuation is properly considered, the location of absorption of the light quanta can be placed in deeper layers. If, for example, one light quanta would be absorbed in the fifth monolayer, the energy absorbed would be enough to throw out all the above molecules forming a shell-crater like formation. But this does not occur because of the energy being carried away in the lattice or the photodetachment effect observed would be at least an order of magnitude larger.

4.6 Wavelength Effects

The experiments on the solid gases ammonia, nitrous oxide, and carbon dioxide were repeated using the 2537Å line of a mercury discharge lamp. The results are given in Table XIV. By comparison, the effects with the 2062Å line as shown in Table XI, are ten to twenty times greater than for the 2537Å line. The intensity of mercury and the iodine lamps respectively were 1.5×10^{15} 2537Å photons/second and 9.6×10^{14} 2062Å photons/second. These values are for

Table XIV

Pressure Change with Valve Closed for 2537Å Line

Gas	$\Delta p \times 10^8$ Valves Closed
CO_2	0.15 ± 0.02
NH_3	<0.1
N_2O	0.11 w/o 9-54 filter 0.5

Source of 2537Å line was a hanovia mercury lamp with a corning 9-54 filter interposed between it and the cell.

equivalent surfaces in square centimeters.

It was expected that the solid ammonia would not show as great a pressure change, indicating detachment, with the 2537Å line as with the iodine persistent line at 2062Å due to ammonia's decreasing absorption coefficient (see Figure 4.13) with increasing wavelength. This effect was nicely illustrated by the decrease from 1.74×10^{-8} Torr pressure change at 2062Å to $< 0.1 \times 10^{-8}$ Torr pressure change at 2537Å.

The carbon dioxide and nitrous oxide both show a decrease in pressure change. This is again consistent with their similarities to each other.

It should be once more emphasized that the substantial decline in effect between 2062Å and 2567Å is not due to the decrease in energy but due to the decrease in absorption coefficient. The absorption coefficient must be in the order of 10^5 or 10^6 or more to be readily observable and giving clear effects. As soon as the absorption coefficient drops to 10^4 or less, only very minor effects can be observed above the background.

4.7 Products of Irradiation

Several attempts were made using the zeolite collection tubes to discover the irradiation products. Table XV gives the results of the product collection.

In all cases, the sample size was extremely small. It was calculated that with the zeolite adsorbing at a very high rate, 10^{17}

Table XV

Irradiation Products

		Products
CO_2	CO_2	
NH_3	NH_3	H_2, N_2 not found
N_2O	N_2O	N_2, O_2 not found

particles per second, the maximum adsorbed would again be dependent on the pumping rate of the MALPHI valve. The calculated value for this is in the order of 3×10^{12} particles per second. If however, one assumes that there is, at any time during irradiation of the solid gas, approximately 3×10^{14} particles available per second, the zeolite at maximum efficiency can collect only one percent. Typically, a collection would be run for 10^3 seconds. This would allow a theoretical maximum of 3×10^{15} particles collected. In terms of pressure, this represents approximately 0.1 Torr. However, the volume concerned in the mass spectrometer and the collection vessel itself at its lowest was in the order of 2×10^2 cubic centimeter. Therefore, the pressure available with maximum adsorption and total desorption would be in the order of 10^{-3} Torr. The total pressure of some experiments ran into mid 10^{-5} Torr range but most were of the order of 10^{-6} Torr.

In addition to the problems associated with working with small quantities of gases, other difficulties such as non-adsorption of a species arises. It was not expected that hydrogen would be adsorbed by the zeolite, and indeed there was no trace found of it. As concerns the gas nitrogen, oxygen, and carbon monoxide, figures supplied by the Linde Company[31] indicate that 5 grams of the zeolite under ideal conditions could adsorb in the order of $10^{21} - 10^{22}$ molecules. The condensible gas can obviously condense within the tube at liquid nitrogen temperatures independent of the zeolite adsorption.

4.8 Temperature Dependence of the Photodetachment Effect

In the limited temperature range, 77°K. to 68°K, of these experiments, there appears to be no temperature effect on the photodetachment phenomena. For all three gases, pressure changes due to irradiation by 2062Å photons and therefore the apparent efficiencies of photodetachment, were not significantly different at 77°K. or 68°K. or any temperature in between.

Part 5

CONCLUSION

The purpose of this work was to investigate under conditions of our solar system, whether molecules, for example, those condensed on comets at large distances from our Sun, could be or would be photodetached.

From the results obtained, the photodetachment phenomena does occur for carbon dioxide, ammonia, and nitrous oxide under these experimental conditions. Further, the effect is both consistent and reproducible within the limits of error. The photodetachment process, for the gases examined, exhibits photodetachment efficiencies in the order of 10^{-4} molecules per photon. Furthermore, the pressure change caused by irradiation with the 2062Å line is directly and linearly proportional to the intensity of the impinging light.

No evidence was found to support the occurrence of a dissociation effect in the solid phase of any of the gases observed. The symmetry of the detachment-recondensation traces support the sampling results which also indicate no dissociation.

The wavelength dependence of the photodetachment phenomena has been demonstrated and related to the absorption coefficient of solid gases presented by other authors.

Doubtless, as extremely low pressures (10^{-12}-10^{-14} Torr) and low temperatures become routine, both the magnitude and character of the photodetachment effect will be more fully investigated. Presently, measurements have to be made at the limit of the available apparatus.

Part 6

LITERATURE CITED

1. Whipple, F.L., Astrophys. J. 111, 375 (1950)
   ibid 113, 464 (1951)

2. Chu, B., Molecular Forces based on the Baker Lectures of Peter J.W. Debye, Interscience Publishers, New York 1967

3. Richter, N.B., The Nature of Comets, Methuen and Co. Ltd., London 1963

4. Zanstra, H., Mon. Not. R. Astr. Soc. 89, 178 (1929)

5. Hughes, A.L. and DuBridge, L.A., Photoelectric Phenomena, McGraw-Hill Book Company, Inc., New York 1932

6. Harteck, P., Reeves, Jr., R.R., and Thompson, B.A., Zeit. Naturforschung 19a, 1 (1964)

7. Herr, D.S., and Noyes, Jr., W.A., J. Am. Chem. Soc. 62, 2052 (1940)

8. Perry, J.H., Chemical Engineers Handbook, (3rd ed.) McGraw Hill Book Company, New York 1950, p. 1548

9. Loeb, L.B., The Kinetic Theory of Gases, (3rd ed.) Dover Publications, Inc., New York 1961, p. 250

10. Lange, N.A., Handbook of Chemistry, (10th ed.) McGraw Hill Book Company, New York 1967, p. 1556

11. Watanabe, K., J. Chem. Phys. 22, 9, 1564 (1954)

12. Zelikoff, M., Watanabe, K., Inn, E.C.Y., J. Chem. Phys. 21, 10 1643 (1953)

13. Inn, E.C.Y., Watanabe, K., Zelikoff, M., J. Chem. Phys. 21, 10 1648 (1953)

14. Wilkinson, P.G., and Johnston, H.L., J. Chem. Phys. 18, 2, 190 (1950)

15. Thompson, B.A., Harteck, P., Reeves, Jr., R.R., J. Geophys. Res. 68, 24, p. 6431 (1963)

16. Mulliken, R.S., J. Chem. Phys. 3, 720 (1935)

17. Sponer, H. and Bonner, L.G., J. Chem. Phys. 8, 1, 33 (1940)

18. Romand, J. and Mayence, J., C.R. Acad. Sci. Paris, 228, 998 (1949)

19. Dressler, K., J. Quant. Spectrosc. Radiat. Transfer 2, 683 (1962)

20. D'Or, L., DeLattre, A., and Tarte, P., J. Chem. Phys. 19, 1064 (1951)

21. Plyler, E.K., Danti, A., Blaine, L.R., and Tidwell, E.D., J. Res. Nat. Bur. Standards A64, 1 (1960)

22. Dressler, K., J. Chem. Phys. 35, 1, 165 (1961)

23. Golding, R.M., Nature 186, 308 (1960)

24. Dressler, K., Schnepp, O., J. Chem. Phys. 33, 1, p. 270 (1960)

25. Granier-Mayence, J., and Romand, J., C.R. Acad. Sci. Paris 236, p. 1148 (1953)

26. Schnepp, O. and Dressler, K., J. Chem. Phys. 32, 6, 1682 (1960)

27. Herzberg, G. and Ramsay, D.A., J. Chem. Phys. 20, 347 (1952)

28. Wood, B.E. and Smith, A.M., AIAA Journal 6, 7, 1362 (1968)

29. Jost, W., Diffusion in Solids, Liquids, Gases, Academic Press, New York 1952

30. Dushman, S., Scientific Foundations of Vacuum Technique , (2nd ed.) John Wiley and Sons, Inc., New York 1962

31. Linde Company Research Laboratory, Reference 5458-28 and 5458-60

Part 7

APPENDIX A

The iodine lamp was found to vary in intensity with distance. Thus it was necessary to characterize its intensity variation. This was done using the ammonia calibration described in section 3.3 while varying the distance from the lamp face to the calibration cell. Figure 7.1 gives the linear variation with distance. Table XVI gives the average value obtained. The triangle designation denotes calibration values made for experimental use as opposed to values obtained for the lamp distance variation. These two types of values coincide within experimental error.

Table XVI

I_2-AR Lamp Variation With Distance
by NH_3 Photolysis Calibration

Distance (cm.)	Intensity (Photons/Sec.) x 10^{-15}
0	5.27
2	1.17
3	0.93
4	0.76
5	0.55

a) Distance measured from cell window surface to lamp window surface.
b) Values of intensity are averages of two or more calibrations.
c) Zero values vary from 9.6 x 10^{15} to 4.0 x 10^{15} indicating a possible plasma coupling interaction.

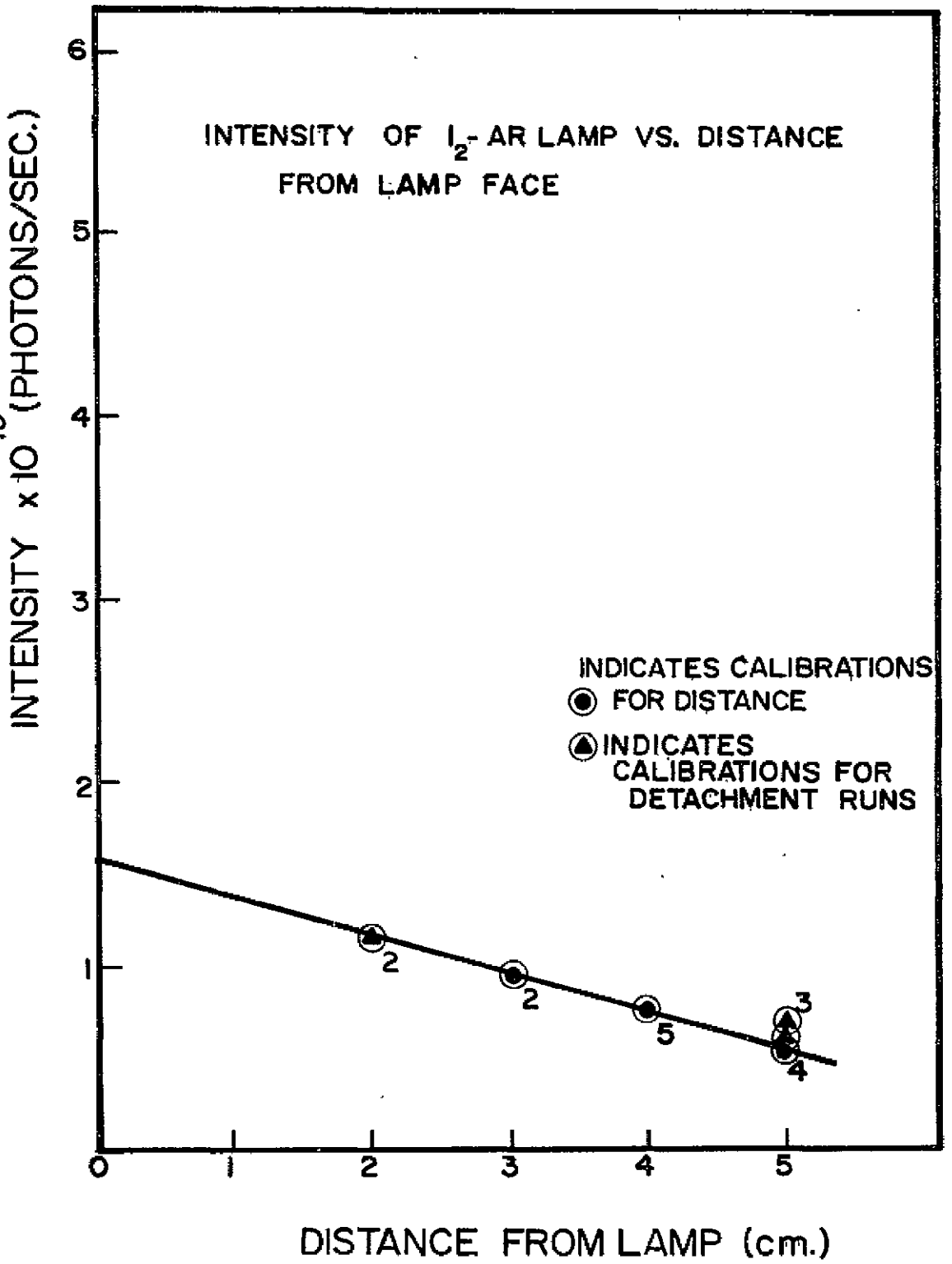

FIGURE 7.1 INTENSITY VARIATION OF IODINE - ARGON LAMP WITH DISTANCE